PLUG NOZZLES: SUMMARY OF FLOW FEATURES AND ENGINE PERFORMANCE

Marcello Onofri
University of Rome "La Sapienza", Roma, Italy
Chairperson of RTO/AVT WG 10 – Subgroup 1

*The text is provided, as originally formatted,
on the following pages.*

	Report Documentation Page	*Form Approved* *OMB No. 0704-0188*

Public reporting burden for the collection of information is estimated to average 1 hour per response, including the time for reviewing instructions, searching existing data sources, gathering and maintaining the data needed, and completing and reviewing the collection of information. Send comments regarding this burden estimate or any other aspect of this collection of information, including suggestions for reducing this burden, to Washington Headquarters Services, Directorate for Information Operations and Reports, 1215 Jefferson Davis Highway, Suite 1204, Arlington VA 22202-4302. Respondents should be aware that notwithstanding any other provision of law, no person shall be subject to a penalty for failing to comply with a collection of information if it does not display a currently valid OMB control number.

1. REPORT DATE **01 JAN 2006**	2. REPORT TYPE **N/A**	3. DATES COVERED **-**

4. TITLE AND SUBTITLE **Plug Nozzles: Summary Of Flow Features And Engine Performance**	5a. CONTRACT NUMBER
	5b. GRANT NUMBER
	5c. PROGRAM ELEMENT NUMBER
6. AUTHOR(S)	5d. PROJECT NUMBER
	5e. TASK NUMBER
	5f. WORK UNIT NUMBER
7. PERFORMING ORGANIZATION NAME(S) AND ADDRESS(ES) **University of Rome "La Sapienza ", Roma, Italy**	8. PERFORMING ORGANIZATION REPORT NUMBER
9. SPONSORING/MONITORING AGENCY NAME(S) AND ADDRESS(ES)	10. SPONSOR/MONITOR'S ACRONYM(S)
	11. SPONSOR/MONITOR'S REPORT NUMBER(S)

12. DISTRIBUTION/AVAILABILITY STATEMENT
Approved for public release, distribution unlimited

13. SUPPLEMENTARY NOTES
See also ADM001860, Technologies for Propelled Hypersonic Flight (Technologies des vols hypersoniques propulses). , The original document contains color images.

14. ABSTRACT

15. SUBJECT TERMS

16. SECURITY CLASSIFICATION OF:			17. LIMITATION OF ABSTRACT	18. NUMBER OF PAGES	19a. NAME OF RESPONSIBLE PERSON
a. REPORT **unclassified**	b. ABSTRACT **unclassified**	c. THIS PAGE **unclassified**	**UU**	**26**	

Standard Form 298 (Rev. 8-98)
Prescribed by ANSI Std Z39-18

AIAA 2002-0584

PLUG NOZZLES: SUMMARY OF FLOW FEATURES AND ENGINE PERFORMANCE
Overview of RTO/AVT WG 10 Subgroup 1

Marcello Onofri
University of Rome "La Sapienza", Roma, Italy
Chairperson of RTO/AVT WG 10 – Subgroup 1

Contributions by:

M.. Calabro, *EADS-LV, Les Mureaux, France*
G.. Hagemann, H.Immich and P. Sacher, *Astrium GmbH, Munich, Germany*
M. Onofri and F. Nasuti, *University of Rome "La Sapienza", Roma, Italy*
P. Reijasse, *ONERA, Meudon, France*

ABSTRACT

This paper represents an overview of the activities carried out in the framework of RTO/AVT Working Group 10, Subgroup 1, dedicated to plug nozzle aerothermodynamics and performance. The subgroup worked out two main objectives: i) thorough understanding of the flow physics of plug nozzles trough literature review and recent experiments conducted in Europe and USA; ii) definition of CFD test cases, conduction of CFD calculations and comparison with experimental data. This paper summarizes the findings of the flow physics based on literature review and recent experiments. It is the result of the many interesting discussions promoted by all members participating to the subgroup, whose contribution is acknowledged by the authors. In particular, the following key topics are discussed in depth in the paper:
- Survey on Past AGARD Activities.
- The Fundamental Aspects of Plug Nozzle Flowfields.
- The Wake Structure Transition from Open to Closed.
- The Influence of the External Flow.
- Plug Nozzle Base Pressure versus Flight Altitude.
- Altitude Adaptive Character of Plug Nozzles with Regard to Performance.
- Contour Design Methods.
- Aerospike: Thrust Vector Control.

NOMENCLATURE

C_F	=	Thrust Coefficient
M	=	Mach number
p	=	Static Pressure

P_0	=	Total Pressure
PR	=	Nozzle Pressure Ratio (p_c/p_a)
r	=	Distance from the simmetry axis
u	=	Velocity
x	=	Distance along the axis
β	=	Mach line angle (characteristic wave, positive clockwise); and thrust deflection angle
ε	=	Area ratio
θ	=	Flow turning angle
φ	=	Plug exit angle
γ	=	Ratio of specific heats
η	=	Efficiency ($C_F/C_{F,i}$)

Subscripts

1	=	Primary Nozzle exit section
∞	=	Free-stream
a	=	Ambient
b	=	Base
c	=	Chamber
d, D	=	Design
e	=	Nozzle exit
i	=	Ideal
int	=	Internal
p	=	Plug
s	=	Shroud
tr	=	Open/Closed wake transition

* Professor, Dipartimento di Meccanica e Aeronautica, Via Eudossiana 18, Roma 00184, Italy, Senior Member, marcello.onofri@uniroma1.it

1. SURVEY ON PAST AGARD ACTIVITIES

prepared by
P. Sacher
Astrium GmbH, Space Infrastructure Propulsion,
Munich, Germany.

The problem of optimizing the afterbody nozzle integration for airbreathing propelled vehicles has been a long time subject of special dedicated efforts within

1

the AGARD technical programs. In view of the new effort of creating again a working group to review the present status of the art and to explore progress having been made since previous activities related to afterbody nozzle and external flow interaction and nozzle afterbody integration, it is worthwhile to shortly summarize at the beginning of this exercise the objectives and the major outcome of the past activities.

In 1972 AGARD initiated a multinational program on improved nozzle testing, the WG 04, in which nine organizations from five nations participated. For a first comparative study, three axisymmetric afterbody nozzle configurations were defined with boattail angles of 10°, 15° and 25° respectively with one internal convergent nozzle contour. The work done was purely experimental the tests covered the Mach number range from 0.6 to 0.95 (1.5) and nozzle pressure ratios of 1 to 7 (15). A major emphasis was given to identify the influence of different test facilities and different model support systems on the boattail pressure distribution. The Results obtained are very well documented in Ref. [1]. Conclusions and recommendations for next activities were:

1. to investigate the effects of exhaust temperature,
2. to redefine and extend analytical procedures to cases with shock wave boundary layer interactions,
3. to develop the use of computational procedures to assess wind-tunnel wall interference and
4. to perform a refinement in wind tunnel calibrations.

In 1984 it was timely to review in a new AGARD WG-08 the progress achieved. Since AGARD has published the results of the WG-04, both wind tunnel techniques had been improved considerably and computational fluid dynamics for drag evaluation and prediction of pressure distributions has reached the status of practical applicability for axisymmetric nozzles even with highly viscous dominated or even partially separated afterbody transonic flow. This new working group assessed specifically[2]:

a). with regard to computational methods
- the status of inviscid methods including jet effects,
- the status of methods for afterbody flow computations including viscous effects (both jet/free stream mixing and boundary layer)
- the status of solutions of the full or thin-layer parabolized Navier-Stokes equations
- the critical range and accuracy of available methods with respect to afterbody drag prediction.

b). with regard to experimental methods
- afterbody testing and testing results since 1975, with special attention to drag/thrust evaluation,

- progress in afterbody testing achieved with conventional jet simulation and with turbine powered simulation (TPS),
- Analysis of wind tunnel test techniques,
- methods to detect flow instabilities and unsteady boundary-layer separation effects including afterbody buffeting and
- wind tunnel correction methods for afterbody tests.

Thirteen test cases were identified. The prime criterion for selection was the availability of extensive experimental measurements of surface pressure and flow field characteristics. Eight of the test cases were typical airplane-type nozzle configurations and the remaining five were typical missile afterbody configurations. In all cases, the jet exhaust was simulated with high-pressure air. Cases were selected to show the effects of nozzle geometry, nozzle pressure ratio, free-stream Mach number, jet exhaust temperature and wind tunnel blockage. All test cases used for CFD comparisons were limited to axisymmetric configurations at zero degree angle of attack.

The general conclusion at the end of the second AGARD WG was that the experimental techniques had reached a very high level of reliability if proper correction procedures are applied and error analysis is performed as recommended. In the area of CFD is was stated, that research and development had reached the level of applicability for simple (single jet) geometry using viscous/inviscid interaction methods or solutions of the Navier-Stokes equations. Both, experimental techniques and CFD are understood now as being complementary tools for the design of optimal afterbody shapes.

In 1992, one decade later, AGARD again felt again its time to provide an update and to review once more the state-of-the-art, now with particular consideration of the progress made on the computational simulation of three-dimensional viscous flow. The specific objectives of AGARD WG17, were[3]:

1. to study 3D aspects of aircraft afterbody integration, that is, at angle of attack, at non-axisymmetric afterbodies and at twin jet configurations,
2. to evaluate present experimental methods and recommend additional techniques as appropriate,
3. to collect databases in order to understand flow physics and to validate computational tools and
4. to calculate 3D afterbody flows to assess the state-of-the-art and to recommended advancements.

WG-17 was organized in two groups, the first, concentrating on the understanding and simulation of the "Fundamental Flow Phenomena" and the second, addressing the wider practicalities of applying such

2

simulations to highly complex geometries typical for advanced fighter aircraft during "Design and Engineering Work".

Group 1: Fundamental Flow Phenomena
Three test cases have been selected to constitute a database allowing an in depth validation of advanced computer codes on basic configurations reproducing typical afterbody flow situations. Only threedimenional configurations and cases with hot gas simulations were considered, the cold jet case being only retained for reference. For all test cases detailed flow field data were available without restrictions:
A.1 Axisymmetric body without jet at incidence 5° at Mach=0.54;
A.2 Axisymmetric body with cold/hot jet at Mach=0.8 and jet expansion ratio of 4.8;
A.3 Twin jet with cold flow at Mach=0.8/0.85 and jet expansion ratio of 5.
Numerical results obtained from Navier-Stokes simulations by seven different organizations and comparisons with experimental data were provided only for testcase A.2.

Group 2: Design and Engineering Work
Semi-empirical and CFD design methods were applied and experimental data were provided for four test cases (each with variants) covering as major variables free stream Mach number, nozzle pressure ratio, aftend shape, tail position and single and twin engines with and without boundary layer separation at the afterbody/nozzle configuration.
B.1. NASA Langley single engine afterbody without tails at Mach=0.9 and PRs =2/5;
B.2. NASA Langley single engine afterbody with two different tails at Mach=0.9 and PRs =2/3/5;
B.3 NASA Langley twin engine afterbody with three different tails at Mach=0.9 and PR=3.4;
B.4. NASA Langley 2-D convergent-divergent single isolated nozzle at Mach=0.6 and 0.94 and PR=4.0.
Numerical results obtained from 14 different organizations are compared with the experimental data mostly with regard to surface pressure distributions and drag coefficients. Recommendations are given for future work.

2. THE FUNDAMENTAL ASPECTS OF PLUG NOZZLE FLOWFIELDS

prepared by
Marcello Onofri and Francesco Nasuti
University of Rome "La Sapienza", Rome, Italy

The plug nozzle is an expansion device including a primary nozzle, whose shape can be quite conventional, and a spike or plug yielding an external expansion. One of the main properties of these nozzles is their peculiar interaction with the external ambient, that is able to avoid the flow separation phenomena that affect conventional bell nozzels. In this sense a key role is played by the expansion fan generated at the primary nozzle lip and on its effect on the pressure behavior along the plug wall. The following contribution analyzes this phenomenon by examples aiming to show the fundamental nozzle behavior. Ideal plug nozzle behavior is analyzed first, with the assumption of full length plug, inviscid gas, quiescent air and plug profile designed as such to provide parallel flow at the design operating condition with axial flow at the plug exit. Maintaining the same assumptions, the analysis is continued for nozzles different than ideal, featuring more practical internal expansions. Finally, some aspects of plug truncation are also discussed.

FULL LENGTH IDEAL PLUG

The analysis of full-length plug configurations is a good reference to evaluate the performance of truncated plug nozzles whose design is based on the same plug geometry. The case here reported features a linear plug nozzle with a sonic orifice as a primary nozzle[4,5], exhausting over an ideal contour plug designed following the Angelino's method[6]; the design nozzle pressure ratio is PR=200, where PR indicates chamber to ambient pressure ratio.

The inviscid solution at design condition (PR=200) is shown by Mach number contours in Fig. 2.1a. Because of the interaction with the lower pressure ambient, the exhaust jet undergoes a centered expansion at the primary nozzle lip, and rotates up to the axial direction. The reflected expansion waves are canceled out by the suitable design of the plug geometry, and eventually uniform axial flow is obtained at the plug exit. The corresponding computed wall pressure is a monotonic decreasing function (Fig.2.2). The profile of the jet boundary is a straight line parallel to the x-axis, as theoretically expected from the plug design. In practice, the nozzle behaves like an ideal nozzle designed for the same PR, for both design and underexpanded conditions. Indeed, it is easy to infer that when the ambient pressure falls below the design conditions, the further expansion at the primary nozzle lip yields no effect on the plug. Thus, in underexpanded conditions, the thrust increases only because of the pressure thrust term, like in conventional underexpanded nozzles, whereas the impulse thrust term remains unchanged.

The advantages of plug nozzles are shown, on the contrary, by its adaptation capability in overexpanded conditions, that makes plug nozzles suitable to achieve very high expansion ratios at altitude.

In fact, when ambient pressure is higher than the design value, the nozzle behavior is again driven by the expansion at the primary nozzle lip. In particular, the exhaust flow undergoes a weaker centered expansion at

3

the primary nozzle lip, and turns less than in design conditions. Therefore, the last expansion wave impinges on the plug wall at shorter and shorter distance from the primary nozzle exhaust section (Fig. 2.1b-h). Downstream of the last expansion wave, the plug geometry, designed such as to avoid the reflection of the other expansion waves occurring for PR=200, generates compression waves. They interact with the jet boundary, yielding its rotation, as shown in Fig.2.1c-h. The result of the interaction of the compression waves with the constant pressure jet boundary is a second centered expansion fan, which makes the flow expands again downstream, where the whole cycle can be repeated. As ambient pressure further increases the expansion at the primary nozzle lip (Fig.2.1c-d) reduces accordingly, leaving larger and larger part of the plug to the expansion-compression, having smaller and smaller amplitude (Fig.2.2).

The self-adaptation process is indicated by the flow at the plug exit section, displaying nearly axial direction, and average pressure nearly equal to the ambient pressure. This behavior is also confirmed by the values, shown in Fig. 2.3, of the nozzle efficiency η, defined as

the ratio of the thrust coefficient (C_F) to the ideal thrust coefficient $(C_{F,i})$. The $C_{F,i}$ is the maximum theoretical C_F achievable at an assigned pressure ratio, computed by one-dimensional (1D) relations (ideal adapted nozzle).

The computed efficiency is high in both on-design and off-design conditions, and its displacement from 1.0 is of the same order of the numerical accuracy of the computations for the whole range of pressure ratios explored. As reference values, Fig. 2.3 shows also the efficiency of conventional nozzles designed for the pressure ratio PR_d, computed by 1D relations. These values allow quantifying the advantages of a self-adaptable nozzle. One of its well-known properties is to show, for the operations at the lower PRs, better efficiency than a conventional nozzle designed for the same PR_d, even without accounting for the well-known troubles of a conventional nozzle in highly-overexpanded conditions. Another is to show, for the operations at the higher PRs, higher efficiency than a conventional nozzle designed for lower PR_d.
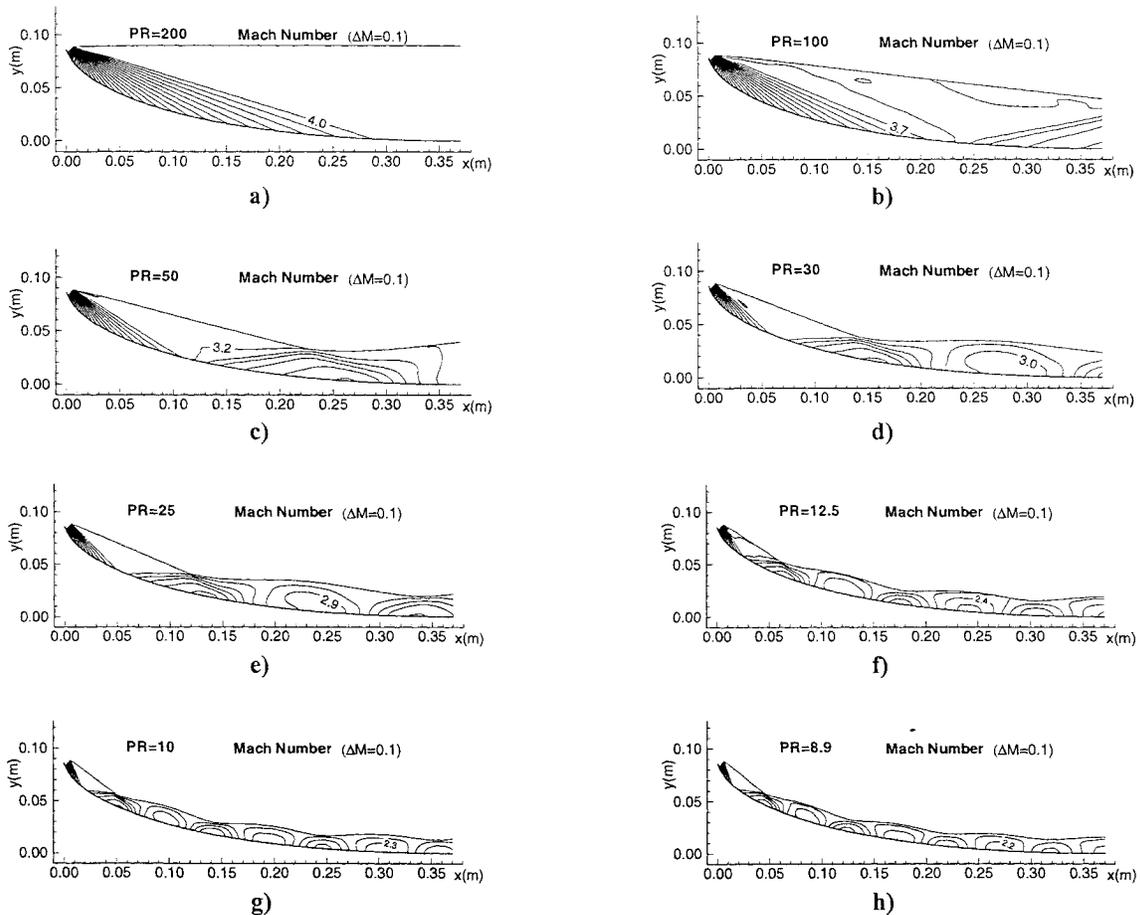
Fig. 2.1: Inviscid computation of full length ideal plug.Mach number contours for different pressure ratios: a) PR=200; b) PR=100; c) PR=50; d) PR=30; e) PR=25; f) PR=12.5; g) PR=10; and h) PR=8.9 [4].

4
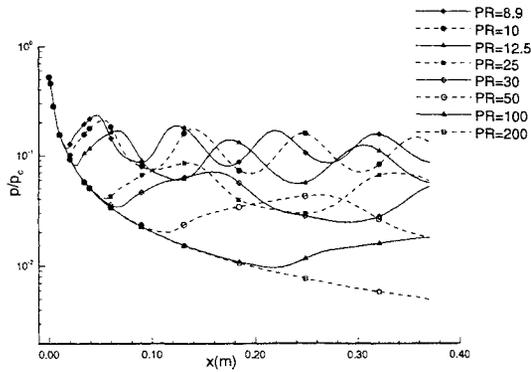
Fig. 2.2: Inviscid computation full length ideal plug. Pressure along the plug wall for different pressure ratio.

FULL LENGTH PLUG WITH SUPERSONIC INTERNAL EXPANSION

To emphasize the role of the primary nozzle geometry on the flow evolution along the plug nozzle and on its

design, a second linear plug nozzle is considered, characterized by a primary supersonic bell nozzle, expanding at pressure ratio PR=28.8. In this case, the non-uniform flow exhausting from the primary nozzle, makes more difficult to design plug geometry capable of canceling out all the impinging waves. An interesting example of these problems is provided by the configuration of the plug extension designed by DASA[5] for a design pressure ratio PR_d=200. It still follows the Angelino's approach, but it is smoothly jointed to the primary nozzle contour.

As shown by Mach number contours in Fig. 2.4a the flow over the plug features many waves, even in design conditions. This depends on several aspects. First, the flow at the exit of the primary nozzle is not uniform, due to the symmetric expansion fans coming from the nozzle throat and to the following compression waves generated by the change of wall curvature downstream of the throat section. Second, these waves interact with the compression waves generated at the exit of the primary nozzle by the concave plug wall curvature.
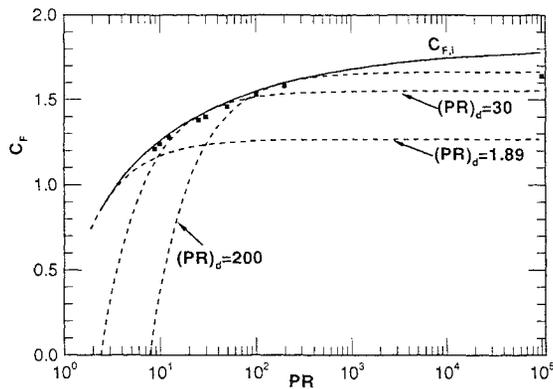
PR	C_F	$C_{F,I}$	η
8.9	1.21	1.23	0.986
10	1.24	1.26	0.982
12.5	1.28	1.30	0.984
25	1.38	1.40	0.984
30	1.40	1.42	0.982
50	1.46	1.49	0.985
100	1.53	1.55	0.984
200	1.58	1.60	0.989

		PR=8.9	PR=30	PR=200	PR $\rightarrow \infty$
Linear Plug Nozzle	(PR_d=200)	0.99	0.98	0.99	0.92
Conventional	(PR_d=200)	0.18[†]	0.86[†]	1.00	0.92
Conventional	(PR_d=30)	0.92[†]	1.00	0.96	0.86

[†] = Conventional nozzle in overexpanded regime. Indeed, a recover due to separation would occur[7], but separated operations are not considered as practical.

Fig. 2.3: Efficiency (η) of full length ideal plug nozzle (inviscid computation) and conventional nozzles (inviscid 1D relations).

The result of these two phenomena is the formation of stronger compression waves emanating from the plug wall, which coalesce in a shock inside the exhaust jet. Finally, further downstream this behavior is canceled out by the expansion waves generated at the primary nozzle lip. All these flow features are more evident if the characteristic net is drawn (Fig. 2.4b).

The result shows also that the jet boundary does not start horizontal. In fact, the expansion at the primary nozzle lip is more intense than the designed one, because the pressure value near the primary nozzle wall is higher than the average exit pressure, which was considered as design condition. Afterwards, as shown by Fig. 2.4b, the jet boundary is bent by the expansion waves coming from the lower side of the throat, and becomes nearly horizontal, until it is reached by the shock wave generated along the plug wall. At this point it turns again upwards, and at the plug exit the flow is still slightly non-axial and non-uniform.

a)

b)

c)
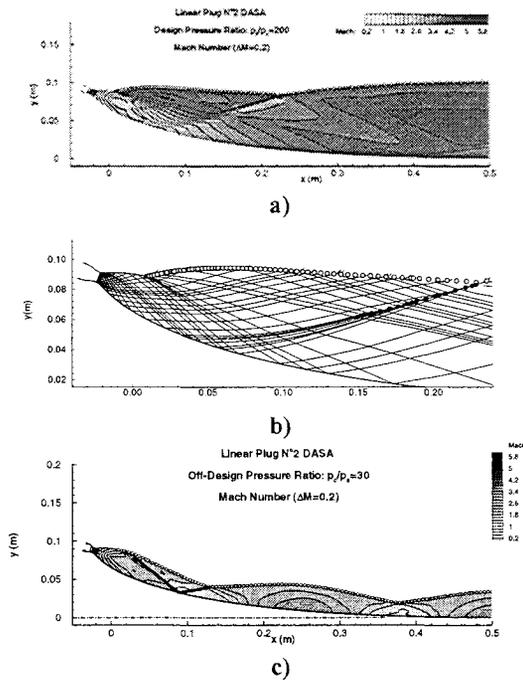
Fig. 2.4: **Inviscid computation of full length plug nozzle with supersonic internal expansion. a) Mach number for PR=200; b) Characteristic net for PR=200; c) Mach number for PR=30. •=shocks, o =jet boundary.**

	PR=30	PR=200
Linear plug nozzle (PR$_d$=200)	0.98	0.99
Ideal linear plug nozzle (PR$_d$=200)	0.98	0.99

Table 2.1: Efficiency (η) of full length plug nozzle with supersonic internal expansion (inviscid computation).

Higher ambient pressures lead to narrower jets, as shown for instance for PR=30 in Fig. 2.4c. This PR value is close to the minimum pressure ratio to be considered in order to have the primary nozzle works in underexpanded conditions. The expansion waves coming from the lower side of the primary nozzle throat section are no longer spread by the expansion fan at the primary nozzle lip as in the case PR=200. This leads to a smaller radius of curvature of the downward turning of the jet, just after the nozzle lip. The consequence is the generation of compression waves more rapidly coalescing in a shock wave. The generation of this shock wave hides the phenomena that led to the shock formation in the case PR=200. In fact, the combined effect of compression waves from the upper side of the throat region and from the concave wall remains unchanged. However, since the new shock impinges on the plug wall just downstream the region where that combined effect occurs, the compression waves leaving the plug wall no longer coalesce in a new shock but strengthen the reflected shock.

As a further comment, the comparison with the foregoing plug nozzle shows that the higher the Mach number at the primary nozzle exit, the easier the compression waves coalesce in shocks. Nevertheless, in spite of the presence of shock waves in the exhaust jet, there is no major consequence on the nozzle efficiency (Tab. 2.1), at least theoretically (inviscid case). However, the occurrence of shocks like those shown in Fig.2.4c is undesired in practical applications, because the shock/boundary-layer interactions may yield bubbles of separated flow, with consequent reduction of performance, hot spots on the plug, and local instabilities.

TRUNCATION OF PLUG NOZZLES

One of the main advantages of plug nozzles is that their performance is not dramatically changed if the plug is truncated at even a small fraction of its length. Indeed, the ending part of the plug (like in the case of conventional nozzles) is fairly flat and its contribution to thrust is a small fraction of the overall nozzle thrust, as the force acting on the plug wall is nearly perpendicular to nozzle axis.

An experimental analysis of truncated nozzle performance has been carried out at DASA within the FESTIP study on the model shown in Fig.2.5. A more detailed discussion on the results obtained is reported in Refs. [5,8]. However, for 20%-plug body, Fig. 2.6 shows Schlieren images and the system of left- and right-running characteristics as computed with the Method of Characteristics (MOC) at two overexpanded pressure ratios. Results of the inviscid method of characteristics compare well with the Schlieren images and emphasise different flow phenomena. At the

6

American Institute of Aeronautics and Astronautics

a)   b)
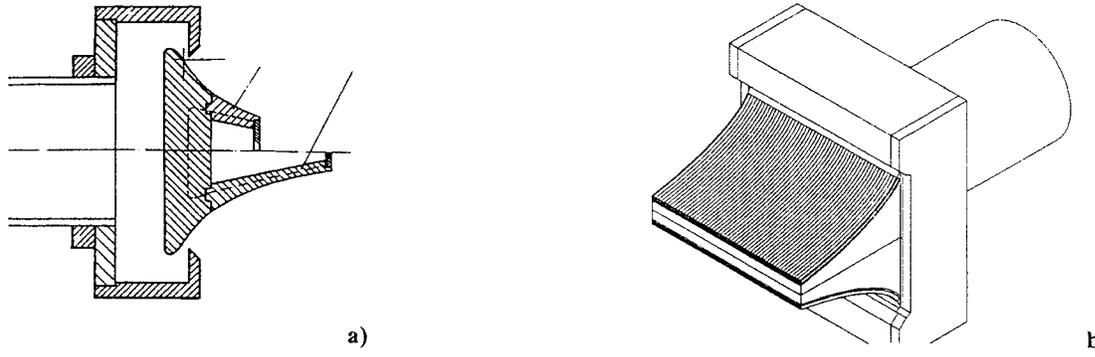
Fig.2.5: Truncated linear plug nozzle tested at DASA within the FESTIP study. a) Section for 10% and 20% truncations; b) three-dimensional view.[5,8]

a)

c)

b)

d)
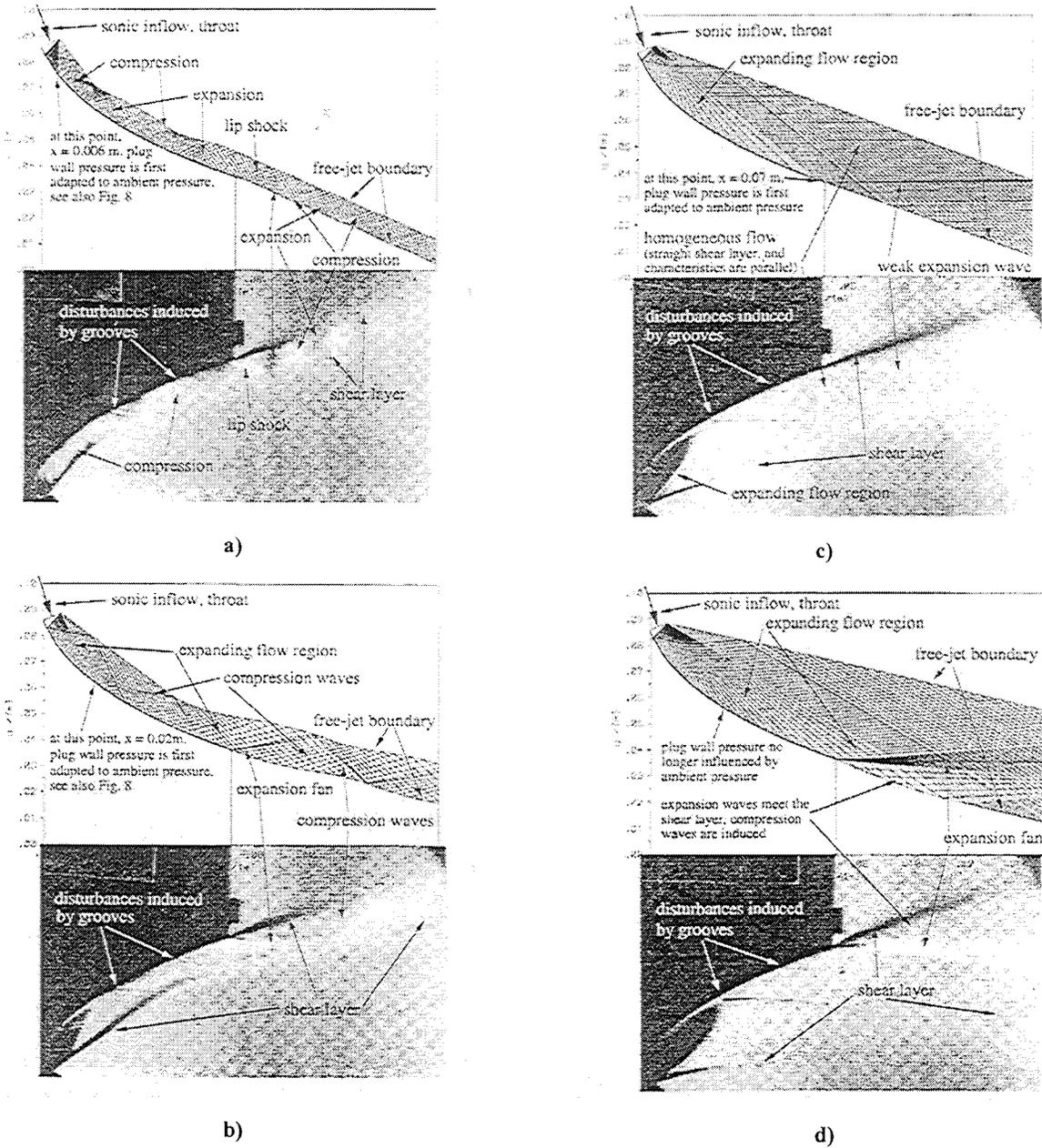
Fig.2.6: Left- and right running characteristics and corresponding Schlieren images for the FESTIP linear plug nozzle. a) PR= 4.2; b) PR =10.4; c) PR = 33.5; and PR = 56.5.[8]

7

American Institute of Aeronautics and Astronautics

10 % Length (inviscid)

PR	C_F	$C_{F,i}$	η
30	1.07	1.42	0.76
200	1.52	1.60	0.95

20 % Length (inviscid)

PR	C_F	$C_{F,i}$	η
8.9	1.09	1.23	0.89
10	1.12	1.26	0.89
20	1.12	1.37	0.82
30	1.21	1.42	0.85
100	1.46	1.55	0.94
200	1.55	1.60	0.97

20 % Length (viscous)

PR	C_F	$C_{F,i}$	η
8.9	1.09	1.23	0.89
20	1.23	1.37	0.89

100% Length: η=0.98-0.99
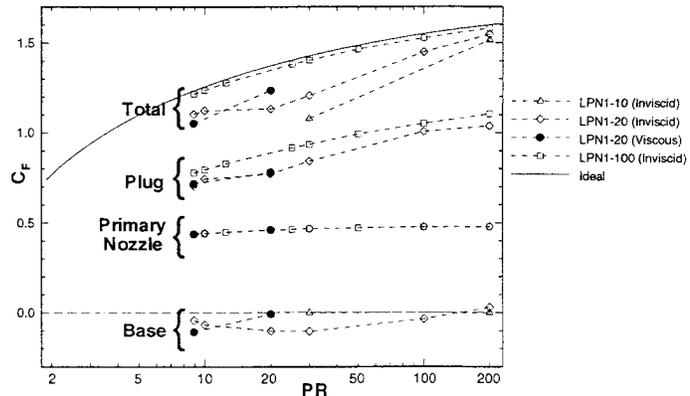
Figure 2.7: Efficiency (η) of plug nozzles truncated at different lengths, as obtained by viscous and inviscid simulations. The value of C_F is split in the contributions of primary nozzle, plug and base in the plot.

lowest pressure ratio PR=4.2 (Fig. 2.6a), a lip shock is centred at the end of the plug body, because the base pressure is higher than the upstream wall pressure. At the pressure ratio PR=10.4 (Fig. 2.6b), upstream wall pressures are higher than the base pressure, and an expansion fan accelerates the flow to the base pressure. At the intermediate pressure ratio PR=33.5 (Fig.2.6c), the plug end wall pressure and ambient pressure are almost equal, and only a very weak expansion is observed. Therefore, the lower shear layer separating the base flow and the supersonic exhaust flow has almost the same slope as the contour at its truncation. Thus, the formation of an expansion wave or a lip shock at the end tip strongly depends on the pressure difference between upstream wall pressure and base pressure.

Some results of the analysis performed by both inviscid and viscous calculations on early truncation (10% and 20%) of the plug nozzles discussed in the foregoing section are summarized in Fig. 2.7. They allow a qualitative analysis of the performance, showing also that the base contribution to thrust ranges from a small drag or a neutral contribution in the overexpanded regime, to positive values at higher PR.

3. THE WAKE STRUCTURE TRANSITION FROM OPEN TO CLOSED

prepared by
Marcello Onofri and Francesco Nasuti
University of Rome "La Sapienza", Rome, Italy

The understanding of the mechanism of transition from open to closed wake in the region behind the truncated base is important for the applications of plug nozzles. Indeed, its knowledge allows the prediction of the transition, from negative to positive, of the contribution of the plug base pressure to the nozzle thrust, and consequently of the nozzle performance along the flight trajectory.

Many experimental and theoretical studies have been performed on the flow evolution behind truncated plugs or more generally behind backward-facing steps. Among them, it is worth to remind the analyses of plug nozzles performed by Sule and Mueller[11], the theoretical considerations about the flow rotation in base regions performed by Weiss and Weinbaum[12], and finally the large number of recent numerical analyses on the backward-facing step problem[13-16].

From the many visualizations reported in those studies it can be noted that there is no clear definition of the transition point between the two wake structures. Therefore, it is useful to establish a definition based on a practical aspect, considering the pressure value that takes place on the base:

- **open wake:** is the flow structure featuring a base pressure depending on the ambient pressure;

- **closed wake:** is the flow structure featuring a base pressure independent of the ambient pressure.

8

For example, the base pressure values (p_b) in different sampling points are displayed in the lowest part of Fig. 3.1 along with the ambient pressure (p_a) and the wall pressure at the plug lip (p_B). Figure 3.1 shows that p_b depends on PR in the range of low values, whereas it becomes constant for higher PRs. Therefore, according to the present definition, the transition of the wake structure occurs at PR~168 for the example shown in Fig.3.1.
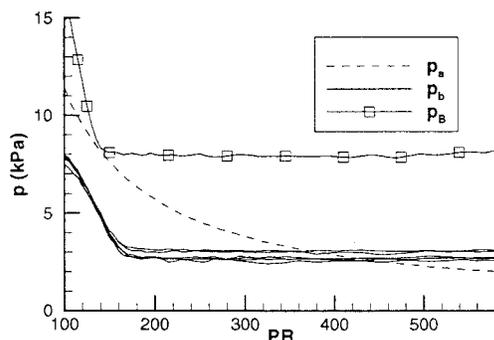
Fig. 3.1: Measured base pressure and plug-exit pressure as a function of PR[17].
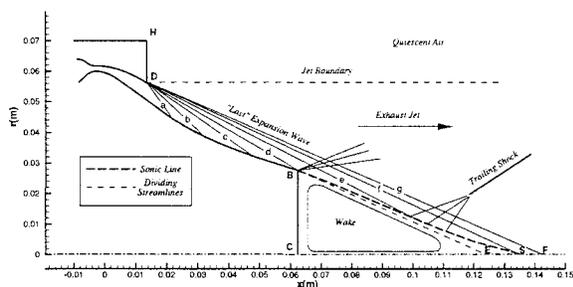
Fig. 3.2: Schematic view of the plug nozzle flow structure (closed wake operation)[18].

It is important to notice that while it is possible to find a wide number of studies on the base pressure prediction, the transition from open to closed wake has not been analyzed in the same depth. The analysis of the flow behavior presented here in the following should provide a greater insight into the main aspects of the wake structure transition.

A schematic view of the flow structure is shown in Fig. 3.2, where the reflected waves possibly generated on the plug surface have been neglected, as well as the mutual interaction among the waves, that is considered as a second order effect.

Independently of the wake shape, of the trailing shock position and of the possible definition of a wake neck (often introduced to evaluate base pressure), it is possible to say that the wake is independent of p_a if the

last characteristic wave g of the Prandtl-Meyer expansion centered in D impinge on the wake downstream of the reattachment point E. This is clear when F, the foot of g, is placed downstream of the sonic point S. In this case, any change in the ambient pressure would only move g inside a supersonic flow, without changing anything in the flow upstream. On the other hand, when F lies between E and S, only a slight effect on p_b is expected, whereas the position of g will certainly affect p_b when it impinges directly on the separated region. Therefore, for increasing p_a, the ambient pressure effect carried by the position of the line g begins to affect significantly the base region only when F reaches the reattachment region around E. The above considerations about the understanding of the closed-open wake transition phenomenon allow to develop suitable engineering models as it will be described in the following.

ANALYTICAL MODEL OF CLOSED–OPEN WAKE TRANSITION

An engineering model developed to predict the pressure ratio PR_{tr} at which the closed-open wake transition occurs[18], is based on the schematic view of the flow structure shown in Fig. 3.2 and discussed in the preceding section. It has to be noticed that only few attempts to model PR_{tr} can be found in the literature[18,33].

The above theoretical analysis has shown that transition should occur when the final expansion wave g, emanating from the lip of the module exit section, impinges in the neighborhood of the reattachment point (E in Fig. 3.2). Therefore, a possible approach to evaluate PR_{tr} may be based on the analysis of the path of g for varying PR.

To evaluate the point F where the wave g impinges on the nozzle axis in the annular plug nozzle case, it has to be noticed that the characteristic lines can no longer be approximated by straight lines, because they are curved by the axisymmetric effect, especially near the symmetry axis. To provide a helpful visualization of that, Fig. 3.3 shows a picture of an enhanced effect of the flow axisymmetry on the curvature of a characteristic line. Compared to the straight line g, the actual line g' corresponds to the larger expansion indicated by the angle β'. Therefore, for an assigned PR, the classic Prandtl-Meyer expansion relations can be used to compute the angle β'. Then the corrected angle $\beta=\beta'+\Delta\beta$ allows to draw the straight line that determines F. The analysis performed in Ref. [18] has shown that constant value $\Delta\beta=5°$ can be assumed in case of annular plug, whereas $\Delta\beta=0°$ in case of linear plug. At this point a model to evaluate PR_{tr} can be easily made available. Indeed, once the position of the point E (i.e. the maximum axial extension of the separated bubble CE) is known, it is possible to

evaluate the corresponding β', and thus PR_{tr}, by inverting:

$$\begin{cases} \beta' = \mu(M_{tr}, \gamma) - \nu(M_{tr}, \gamma) + \nu(M_e, \gamma) + \theta \\ M_{tr} = \left[\frac{2}{\gamma - 1} \left(PR_{tr}^{(\gamma-1)/\gamma} - 1 \right) \right]^{0.5} \end{cases} \quad (3.1)$$

where ν is the Prandtl-Meyer function, μ is the Mach angle, and θ the flow direction at the primary nozzle exit. There are different possible ways to evaluate CE. For instance in the axisymmetric case, following Ref. [71,72], the bubble extension of a supersonic backward-facing step seems to be independent of the approaching flow Mach number[71] for M>2 and its value[72] such that CE~2.65×BC.
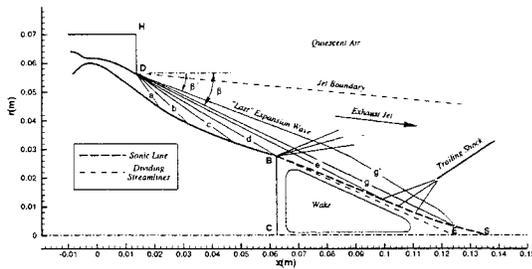
Fig. 3.3: Schematic view of the simplified model of characteristic lines at closed--open wake transition[18].

The comparison with experimental data carried out in Ref. [18] indicated that to evaluate CE a correction should be introduced in the above relation to consider the departure from a backward-facing step case. The most effective parameter to achieve this correction, has been found to be the plug exit angle (φ), that is the wall slope at B with respect to the axis. This analysis suggested to use for annular plug nozzles the following correlation that assumes the value CE/BC=2.65 when φ=0° according to Ref. [72]:

$$CE/BC = 2.65 - 0.00144\varphi^2 \quad (3.2)$$

Some results obtained by the present model and compared to experimental data are reported in Tab.2.2.

Source	N	Length	φ	PR_{tr} Model	PR_{tr} Exp.
Ref.17	24	40.0%	10°	166	168
Ref.17	24	20.0%	14°	117	112
Ref.17	24	5.0%	20°	78	73
Ref.17	12	40.0%	10°	155	165
Ref.17	12	20.0%	14°	108	108
Ref.17	12	5.0%	20°	72	77
Ref.27	12	20.0%	18°	38	40
Ref.78	24	9.4%	13°	129	130
Ref.78	24	0.0%	18°	96	100

Table 2.2: Prediction of PR_{tr} by the present model and compared to experimental data for clustered modules plug nozzles (N=number of modules)[18].

It is worth to notice that the results of the present model shown in Tab.2.2 the case of annular clustered module plug nozzles, where the effects of dissymetries due to clustering can be reasonably neglected in the base region. Some other models for transition from open to closed wake be also found in the literature[18,33].

4. THE INFLUENCE OF EXTERNAL FLOW

prepared by
Marcello Onofri and Francesco Nasuti
University of Rome "La Sapienza", Rome, Italy

The external flow surrounding the plug nozzle during its flight operation may noticeably affect its performance, because of local changes of the ambient properties, as seen by the exhaust jet.

The comparison of the Mach number flowfield around the whole plug nozzle, including the plug base, with that obtained in case of still air at the same PR emphasizes the slipstream effect. It can be helpful to look at the ambient pressure isobars displayed over the flowfield by a thick dashed line in Fig. 4.1. The still air solution shows that the base pressure is nearly equal to the ambient pressure. In particular, the ambient pressure isobar impinges on the plug wall and, downstream, the remaining part of the plug acts as a compressing surface. It can be seen that downstream of the ambient pressure isobar the flowfield shows nearly constant pressure, that acts also on the base flow region. Only at the wake neck the flow must compress and the pressure becomes higher than ambient. On the contrary, in the M_∞=2 case, the driving mechanism of the expansion is the shroud base pressure value, that is lower than the ambient pressure. Therefore, the expansion covering the plug wall continues downstream the ambient pressure isobar, so that a part of the plug and the base are affected by pressure lower than ambient.

Therefore, as also stated above, the M_∞=2 solution represents a typical case of closed wake behavior, with a base pressure value independent of p_∞ for increasing PR, whereas open wake with $p_b \sim p_\infty$ is shown in case of still air. This different behavior at the same PR indicates that a different mechanism drives the transition from open to closed wake.

In the still air case, it has been shown in the foregoing section[18] that transition takes place when the last characteristic wave emanating from the primary nozzle lip impinges on the nozzle axis ahead of the stagnation point region. Conversely, in the in-flight case the same role is played by the internal shock, that represents the boundary of the expansion process emanating from the shroud base and thus is the first and closer to the plug

10

signal that carries information about the ambient pressure value.

As a consequence, in the case of external stream the indicator of the influence of the external ambient is the internal shock rather than the last characteristic line of the lip expansion fan. Therefore, the engineering model introduced in Ref. 18 for the approximate prediction of the impingement point of the first signal carrying the ambient pressure information should be adequately extended to the case of in-flight operations.
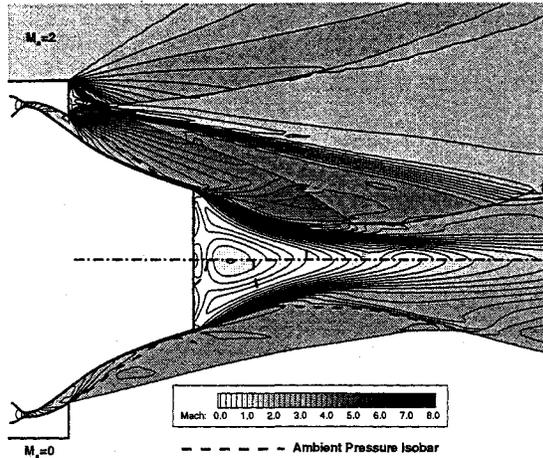
Fig. 4.1: Comparison of supersonic and still air cases[40].

The main consequence of the behavior illustrated above is to move the open/closed wake transition point towards lower values of PR, with the consequence that the overall performance (without accounting for the shroud effect) is reduced especially in the range of PR between the expected value of transition in still air and the actual transition value, because in this range the earlier closure yields base pressure lower than ambient. Moreover the present results show also that the shroud shape plays a role in the determination of the transition between closed and open wake.

EVALUATION OF FLOW EVOLUTION ALONG THE FLIGHT PATH

Further interesting effects of the external flow can be seen by the analysis of the flowfield at varying free-stream Mach number[40], passing from zero to subsonic values, then to supersonic, and finally to different values in the supersonic regime. The analysis is carried out by reducing the Mach number in the supersonic range from the highest value considered, while keeping constant the exhaust gas properties and the ambient pressure.

The main effect of reducing M_∞ is the increase of the shroud base pressure, because of the enlargement of the dead-air region with the two counter-rotating vortices and of a lower expansion of both the exhaust jet and

the external stream (Fig. 4.2). In particular, weaker expansions of both jets at the primary nozzle and shroud lips result in smaller flow rotations (smaller *lip rotation angle* in Fig. 4.2), and also in lower Mach numbers of the two jets at the stagnation point. These lower Mach numbers upstream of the stagnation point yield larger angles between the *realignment shocks* and the *dividing streamline*.
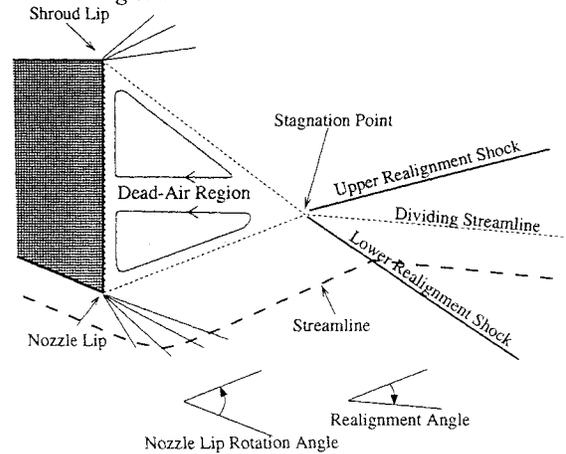
Fig. 4.2: Schematic view of the main flow features about the shroud base[40].
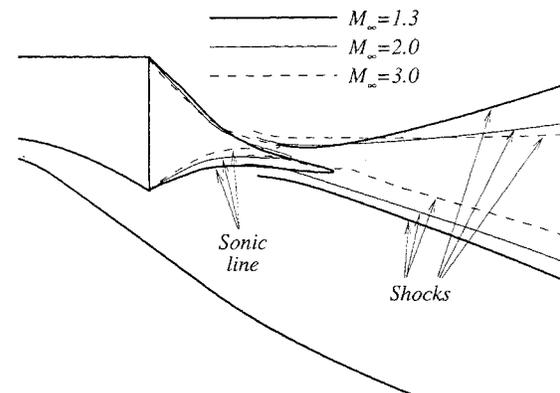
Fig. 4.3: Computed streamlines and shocks about the shroud base for $M_\infty=1.3$, 2.0, 3.0; PR=61.7[40].

Actually, it should be noticed that the final direction of these shocks is affected also by the smaller *realignment angles* to turn back the jets downstream of the stagnation point. Indeed, since the average jet direction downstream of the interaction with the external stream (the *dividing streamline* in Fig. 4.2) mainly depends on the overall pressure ratio, and it is nearly independent of the external Mach number (i.e. also of the shroud base pressure), smaller *lip rotation angles* require smaller *realignment angles*. Nevertheless, it can be seen that the variation of the realignment angles has only a slight effect on shock angles, whose variation is mainly due to the changes of Mach numbers at the stagnation point, upstream of the interaction.

The computed profiles of realignment shocks are shown for three different supersonic Mach numbers, along with the extension of the dead-air region and the final jet direction, in Fig. 4.3. The result confirms that the shocks depart from each other, as M_∞ decreases, because of the lower expansion about the shroud base for both supersonic streams. The main consequence is that the lower shock angle increases its module and consequently will impinge on the wake at lower abscissas. The computations confirm that the jet direction after interaction is almost insensitive to M_∞, but they also indicate that there is a translation of the dividing streamline towards the plug, that yields a further inner displacement of the internal shock for decreasing M_∞.

These considerations may become important when trying to develop a model for the prediction of open/closed wake transition, because -- as mentioned above -- the shock is the first wave carrying the ambient pressure information to the base region.

The further reduction of Mach number from supersonic to subsonic values yields a major change in the flow structure behind the shroud. In fact, the plug nozzle flowfield in subsonic flight conditions is quite similar to the case of still air. Only a slight overexpansion of the exhaust jet takes place in the case of $M_\infty=0.7$ shown in Fig.4.4a, although the external jet becomes locally supersonic because of its expansion at the shroud lip. In the subsonic case the recirculating region at the shroud base is quite large and is dominated by the upper, clockwise-rotating vortex, whereas in the supersonic case the separated region is smaller and is dominated by the two counter-rotating vortices having similar dimensions. Both structures agree with experimental data obtained for similar test cases in Ref. [73] for the subsonic case and in Ref. [74] for the supersonic case, respectively.

M_∞	p_{sb}	p_{pb}	Wake
0.0	12800 Pa	11568 Pa	Open
0.7	9261 Pa	16160 Pa	Open
1.3	1348 Pa	7074 Pa	Open
2.0	713 Pa	5206 Pa	Open
3.0	404 Pa	4543 Pa	Closed

Tab. 4.1: Computed value of average pressure on the plug and shroud bases: $p_\infty=12800$ Pa, PR=61.7[40].

Concerning the plug base, it can be noticed that the raise of shroud base pressure for decreasing Mach number changes the features of the interaction between ambient and plug base region (see Fig. 4.4 and Tab. 4.1). In fact, the wake is clearly closed at $M_\infty=3$, because the internal shock impinges on the wake when it has already become supersonic.

On the other hand, it cannot be considered closed at $M_\infty=2$, as shown in Tab. 4.1 by the increased average pressure value on the plug base, in comparison to

$M_\infty=3$. However, it can be noticed that despite the open wake structure, the average base pressure is considerably lower than ambient pressure. This is because the average pressure in the exhaust jet bounding the wake is lower, due to the overexpansion at the shroud, and the internal shock impinges only on the downstream part of the wake. A further decrease of M_∞, still in the supersonic range, yields a regression of the internal shock with consequent increase of plug base pressure ($M_\infty=1.3$), although the influence of shroud still makes p_{pb} lower than p_a.

a) $M_\infty=0.7$

b) $M_\infty=1.3$

c) $M_\infty=2.0$

d) $M_\infty=3.0$
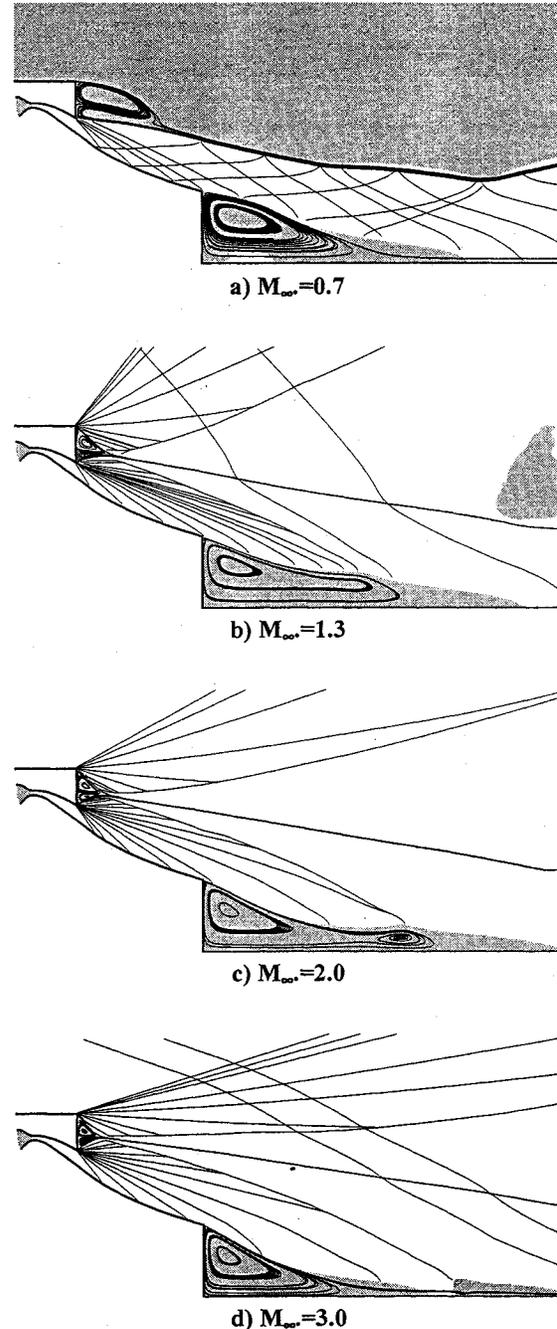
Fig. 4.4: Truncated plug nozzle flowfield in flowing airstream: subsonic regions (filled areas), characteristic waves, closed and dividing streamlines (PR=61.7)

12

A different behavior is shown in the subsonic case, where the average base pressure on the shroud is closer to the ambient pressure value. The consequence is that the exhaust jet does not overexpand significantly, like in the case of still air, and thus there is a direct influence of ambient pressure on the wake.

5. PLUG NOZZLE BASE PRESSURE VERSUS FLIGHT ALTITUDE

prepared by
Philippe Reijasse
ONERA, Meudon, France

In reference to the full-length aerospike nozzle, the determination of thrust budget of a truncated plug nozzle necessitates to solve the additional question of the plug base pressure. It has to be emphasized[4] that for plug length such that the base height is small compared to the total plug height, the contribution of base pressure is negligible with respect to the overall thrust of the nozzle. Furthermore Navier-Stokes computations[29] have shown that even for a 20% truncated plug nozzle, base drag should represent only 5% of the total thrust (inner nozzle, plug and base) at high nozzle pressure ratio (PR).

PLUG NOZZLE BASE-FLOW REGIMES

At low altitude -or low PRs-, ambient pressure is high and greater than the nozzle static pressure at the (cowl) lip. The outer free jet boundary is close enough to the nozzle, and compression waves strike on the nozzle contour and the inner shear layer, see Fig.5.1a[19]. The compression waves impinging on the nozzle contour increase the nozzle wall pressure. The compression waves impinging on the inner shear layer surrounding the subsonic region increase the nozzle base pressure.

As altitude increases, or ambient pressure decreases, compression waves move down the nozzle contour. When ambient pressure becomes lower than the nozzle lip pressure, expansion waves form and are followed by an internal shock which no longer strike the plug contour. In that case, see Fig. 5.1b, the pressure profile along the nozzle contour remains constant with further decreases in ambient pressure. The nozzle base pressure, however, remains under the influence of ambient pressure as long as the internal shock impinges on the inner shear layer surrounding the subsonic region.

At high PRs, when the internal shock moves downstream of the sonic line in the wake of the base flow, see Fig. 5.1c, the decrease of ambient pressure does not affect the nozzle base pressure. Once the base pressure becomes insensitive to the ambient pressure, the aerospike flow regime is called *'closed wake' regime*. Prior to this point, while the nozzle base

pressure is sensitive to the ambient pressure, the aerospike is in the *'open wake' regime*.

We have to take care with this wake regime designation, closed or open, because it concerns only the sensitivity of base pressure versus the ambient pressure for truncated plug nozzle application. Thus the designation of these regimes is totally de-correlated with the recirculation flow pattern. This sensitivity to ambient pressure has been well experimentally identified for different types of plug nozzle configurations[19,20,27], annular or linear, clustered or not. Hagemann[8] had proposed a way to determine the transition point from an open wake to a closed wake thanks to the Method of Characteristics. This transition should occur when the right-running characteristic issued from the nozzle lip intersects the separated shear layer at the foot of the trailing shock. This method when applied to a linear aerospike[21] shows a relatively good agreement and slightly underestimates the transition point, see Fig.5.2.
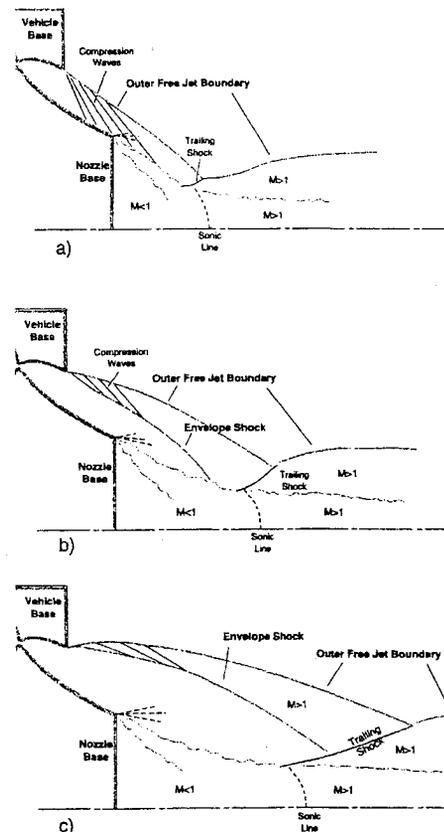
Fig. 5.1 - Plug nozzle flowfields : a) at low PR, b) at intermediate PR, c) at high PR[19].

Indeed, in the case of plug nozzle configuration analysed in Ref. 19, a *closed recirculation bubble* occurs at all PRs. It means that a vortical region is bounded by the nozzle base surface and the inner shear layer which reattaches itself downstream of the base. The reattachment region starts the development of a supersonic thick wake on the centerline. So, the so-called open wake regime of truncated plug nozzles - in

13

terms of base pressure insensitivity to ambient pressure - can even occur when a closed recirculation bubble forms downstream of the base.
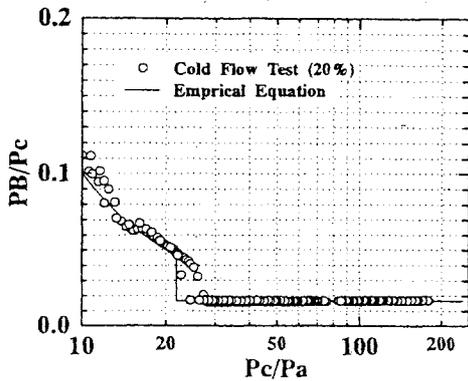
Fig. 5.2: Normalised base pressure versus PR. Experimental data from a linear aerospike nozzle cold gas model[21] compared with Hagemann's assumption[8].
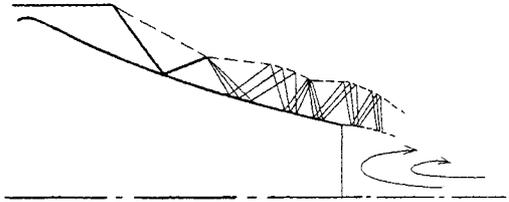
Fig. 5.3: Subsonic open wake flow pattern downstream of a truncated plug nozzle base.

Furthermore, it is also possible that the separated inner shear layer does not reattach itself downstream of the base surface. This could be the case of a truncated plug nozzle with a large base surface comparatively to the annular section of the incoming supersonic jet, see Fig. 5.3. In such a base flow pattern, there is a *subsonic open wake* -really opened this time in terms of fluid mechanics-, and the base pressure is close to the ambient pressure. Thus, in that case, the problem is not to determine the base pressure, but to predict at which value of p_c/p_a the transition 'opening-closing' of the recirculation bubble occurs.

If the base flow pattern is a closed recirculation bubble, whatever the plug nozzle wake regime -closed or open-, then the determination of the base pressure in supersonic regime is submitted to the same flow physics, namely the physics of the *'Supersonic Turbulent Flow Reattachment'*. Motivated by the base drag prediction not only for truncated plug nozzles but mainly for projectile and missile applications, the supersonic base flow physics have been extensively investigated in the world since the 50's. Thanks to many investigations performed downstream of the base of two-dimensional backward-facing steps, it has been derived analytical, pure-empirical and theoretico-empirical models as those presented below.

BASE PRESSURE PREDICTION

Pure empirical relationships

Fick et al.[20] have evaluated empirical relations of the base pressure versus constant incoming Mach number M_e and specific heat ratio. A comparison with the few available measurements showed that the two empirical relations issued from Ref. 30, see Eqs (5.1) and (5.2) below, failed to produce reliable results.

$$p_b = \frac{0.846 p_e}{M_e^{1.3}},\qquad (5.1)$$

$$p_b = p_e\left(1 - 0.715\gamma\frac{M_e^{2.3} - 0.92 M_e^2 - 0.03}{M_e^{2.7}}\right).\quad (5.2)$$

A slighly better agreement was found[20] notably for 12-16% plug lengths if it was assumed that the base pressure results from a very simple averaging between pressure p_e at the truncated nozzle exit and pressure p_d at the exit of the hypothetical design full-length plug, as written below :

$$p_b = k\left(p_e + p_d\right);\quad with\ k = 0.5 .\quad (5.3)$$

When applied to linear aerospike nozzles, it was found[21] that the constant k had to be changed from 0.5 to 0.3 according to measured data.

Derived from cylinders and cones, an original empirical base-pressure model[31] has been changed in Ref. 20 by setting an exponent which should take into account the negative angle of the flow incoming the base region. For cold flow tests, and setting the exponent at 0.35, agreement with measured base pressure has been attainable with the "conical-approximation" equation below,

$$p_b = p_e\left(0.025 + \frac{0.906}{1 + \frac{\gamma - 1}{2} M_e^2}\right)^{0.35}.\quad (5.4)$$

The empirical model derived in Re. 20 from a cylinder embedded in supersonic flow also gives a good agreement if Mach number M_e and a sonic pressure ratio are introduced, thus we obtain the "cylindrical-approximation" equation below,

$$p_b = p_e M_e\left(\frac{2}{\gamma + 1}\right)^{\frac{\gamma}{(\gamma-1)}}\left(0.05 + \frac{0.967}{1 + \frac{\gamma - 1}{2} M_e^2}\right)$$

$$(5.5)$$

Onofri et al.[32] have also evaluated Eqs. (5.4) and (5.5), and another plug nozzle base model proposed by

Rocketdyne, see Eq. (5.6) below*, and compared them with a new formula, see Eq. (5.7) below, applied to a clustered plug nozzle.
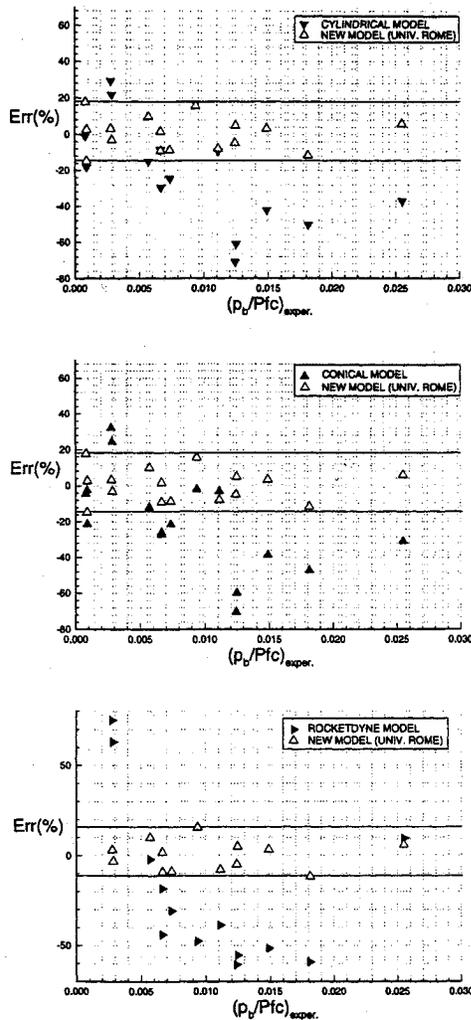
Fig. 5.4: Comparisons between base pressure purely-empirical relationships.

$$\frac{p_b}{p_c} = 0.58 \frac{C_{F,\max,d} - C_{F,core}}{\varepsilon_b} \qquad (5.6)$$

$$p_b = p_e \left(0.05 + \frac{0.967}{1 + \frac{\gamma-1}{2} M_e^2} \right)^{\Phi}, with \qquad (5.7)$$

$$\Phi = \frac{-0.2\phi^4 - 5.89\phi^2 + 20179.84}{\phi^4 + 20179.84}$$

* In eq. (5.6) $C_{F,\max,d}$ indicates the ideal thrust coefficient at the design PR, $C_{F,core}$ the ideal thrust coefficient corresponding to the expansion ratio achieved at the transition point and ε_b the ratio between base and throat areas.

The results of this comparison, see Fig. 5.4, conclude that the model proposed by Univ. of Rome gives the smallest percentage of error [+19%,-15%] relatively to measured data.

The multi-component base-flow model

Preliminary remark

This theoretical approach is based on the flow partition into several regions or subdomains (viscous or inviscid) which are determined thanks to analytical and integral relationships. Flow subdomains are physically linked by semi-empirical relations, and the unicity of the solution is insured thanks to the using of a reattachment criterion. Such methods are able to predict the base pressure in various base configurations[24-26], and notably in case of truncated plug nozzles[26], with the two following reservations: 1) the computed configurations are two-dimensional, planar or axisymmetric, and 2) the base flow region is a closed recirculating-flow bubble. The following chapter is devoted to a brief description of these theoretical approaches, called multi-component methods.
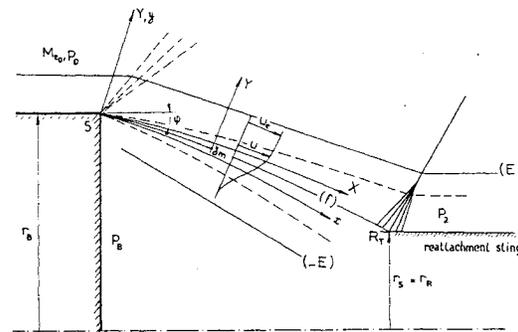
Fig. 5.5: Multi-component base flow model.

Model description

This model is derived from the well-known Korst model[22] for the supersonic separated flow reattaching behind a rearward facing step. As shown in Fig. 5.1a, the basic situation is that of a supersonic turbulent flow separating at a base shoulder S and reattaching further downstream on a wall or a sting in the vicinity of a point F. Mass injection at low velocity (base-bleed) can be performed in the dead air region.

In the spirit of this so-called Multi-Component approach, the flow is divided into four components or domains, Fig. 5.5:

a - The **outer inviscid flowfield** bounded by the isobaric boundary (f) along which the pressure is equal to the base pressure p_b. This boundary intersects the reattachment surface at the "ideal" reattachment point R_T. This supersonic outer inviscid flow can be computed by the Euler equations solved by the Method of Characteristics.

15

b - The *rapid expansion of the boundary-layer* when it separates at base shoulder S. This flow expansion can be treated by a Prandtl-Meyer expansion if we assume the viscous terms influence are negligible in such a process.

c - The *turbulent mixing-layer* developing from the separation point S along the isobaric boundary (f). Transfers of momentum, mass and energy between the outer high velocity stream and the closed recirculation bubble take place in this mixing layer. The velocity distribution across the turbulent mixing-layer is represented by the classical relationship:

$$\frac{u}{u_e} = \frac{1}{2}\left(1 + \operatorname{erf}(\chi)\right), \qquad (5.8)$$

where χ is a similarity variable. The distributions of stagnation enthalpy and species concentration are deduced from the velocity distribution by assuming Prandtl number and Schmidt number equal to unity.

d - The *reattachment region* where the mixing layer impinges on the reattachment surface, the outer flow being simultaneously deflected in such a way so that it becomes parallel to the surface. This deflection entails the formation of compression waves which focalize into the reattachment shock. A compatibility condition at the reattachment point have to be expressed via an empirical criterion. Onera has developed the concept of Angular Reattachment Criterion introduced by Carrière and Sirieix[23]. This angular criterion states that the isobaric outer flow deflection, ψ, at reattachment point must satisfy a law given by semi-empirical relationships[23-25].

The above four domains are thus represented by simplified models and patched together in order to satisfy appropriate compatibility conditions. The main unknown quantities of the problem, notably the base pressure p_b and the dead-air temperature T_m, are then determined by satisfying global conservation equations for mass and energy written for a control volume encompassing the isobaric dead-air region, see Fig. 5.1c.
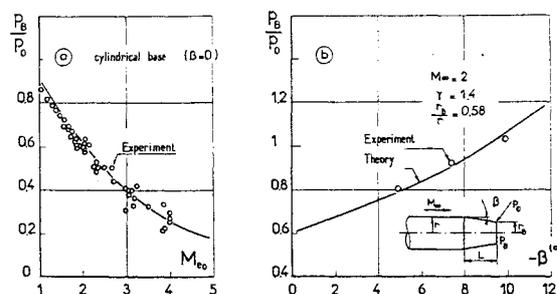
Fig. 5.6: Axisymmetric base pressure predicted by multicomponent theory[25] versus incoming Mach number and boattail angle.

The above basic model has been validated (see Figs. 5.6), on generic axisymmetric base configurations[25], and can be also applied to the base geometry of a truncated plug nozzle[26] if we know exactly the characteristic line -or Mach line- issued from the shoulder of the truncated plug base. This incoming Mach line in the supersonic jet, which initializes the multicomponent model, is generally different from a straight line which should indicate a constant incoming Mach number M_e. This latter assumption, mostly wrong for truncated plug nozzle configurations particularly in overexpansion flow regimes, thus leads to a miscalculation of the outer flow deflection at reattachment point, then to a significant error on base pressure. This error can be amplified in case of clustered plug nozzle configurations, where the three-dimensional aspects cannot be rigorously taken into account in these multicomponent models. Thus the reliability of clustered plug nozzle computations by multicomponent methods relies on the way to determine a mean incoming flow initializing the model.

In conclusion, in case of closed recirculation bubble downstream of a plug nozzle base, reliable predictions of base pressure can be obtained by the multicomponent theoretical approach, more particularly in cold gas configuration and with the reservations the model is initialised with the exact incoming Mach line. Furthermore the influence of base-bleed on plug nozzle base pressure[20, 28], can be also calculated by the multicomponent model, as it has been presented in Ref. 25, 26 for projectile base-bleed applications.

6. ALTITUDE ADAPTIVE CHARACTER WITH REGARD TO PERFORMANCE

Prepared by
Gerald Hagemann, and Hans Immich,
Astrium GmbH, Space Infrastructure Propulsion,
Munich, Germany

The aerodynamic mechanism of altitude adaptation of a plug nozzle has been explained in Section 2. For an ideal plug nozzle with full-length central body, this mechanism finally results in an almost ideal thrust performance vs. altitude over a certain altitude range. As an example, Fig.6.1 shows computed performance data for a toroidal plug with ideal length central body. Its design parameter are included in Table 6.1. Corresponding data for a conventional bell-type nozzle with equal design parameter are included for comparison.

At the altitude corresponding to the design pressure ratio, losses induced in both, in the conventional nozzle and in the plug nozzle, are induced due to internal loss effects, i.e. chemical non-equilibrium, friction, and divergence losses (sector 2 in Fig.6.1). The positive

effect of altitude adaptation is indisputable; for pressure ratios below the design pressure ratio, the plug nozzle performance is practically equal to the theoretical ideal expansion. For pressure ratios higher than the design pressure ratio, the plug nozzle behaves as a conventional nozzle, the loss in altitude adaptation included (sector 3).

The truncation of the central plug body, which is of advantage due to the huge full-length and high structural masses of the contoured central body, results in a different flow and performance behaviour compared to the full-length plug nozzle. This has been discussed in detail in Section 2.

Chamber pressure	$p_c = 100$ bar
Propellants	hydrogen / oxygen
Mixture ratio	$o/f = 6$
Geometrical area ratio	$\varepsilon = 55$

Table 6.1: Design parameter of toroidal plug nozzle and reference bell nozzle used for computations.

At lower pressure ratios an open wake flow establishes, with a pressure level practically equal to the ambient pressure. At a certain pressure ratio close to the design pressure ratio of the full-length plug nozzle, the base flow suddenly changes its character and turns over to the closed form, characterised by a constant base pressure. At the transition point the pressure within the wake approaches a value which is below ambient pressure, and the full base area induces a negative thrust. This thrust loss depends on the percentage of truncation and the total size of the base area. Published experimental data and numerical simulations revealed an increasing thrust loss for shorter plug bodies, since the total base area increases.

Base pressures during open wake condition may be influenced by base bleed injection. Former experiments have shown that a small amount of bleed gas, i.e. ~1% of total mass flow rate, expanded into the base area slightly increases the base pressures during open wake conditions, and thus has a positive influence on the plug performance efficiency, see e.g. Ref. 45.

Performance data of a numerically simulated truncated plug nozzle are included in Fig. 6.2 and compared to the same plug nozzle with full-length central body and a conventional bell nozzle as shown in Fig. 6.1. Design parameter of this truncated plug nozzle are the same as for the full-length plug, see Table 6.1. The thrust loss at a certain altitude where transition in wake behaviour occurs, becomes obvious. Its value of course depends on the real base pressure loss, in the numerical simulations based on quasi-steady state simulations, a pressure loss of approx. 15% was predicted.
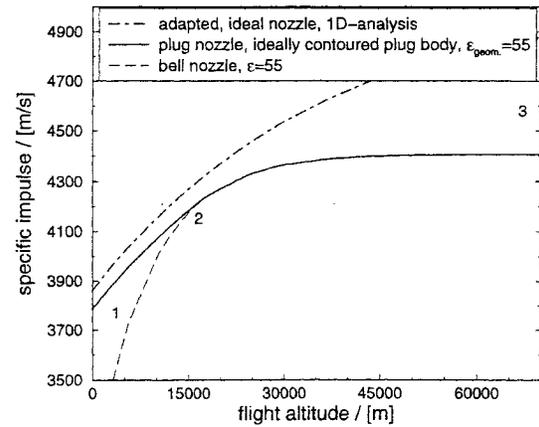
Fig. 6.1: Performance characteristic of an ideal plug nozzle and a bell-type nozzle. Ideal expansion into ambience included for comparison.

The principle of performance characteristic calculated with these numerical analyses are confirmed / proven by experiments, see e.g. Wasko[45].

The performance of plug nozzles is adversely affected by the external air stream flow, i.e. the aspiration effect of the external flow reduces slightly performance and also favours an earlier change in wake flow development for truncated plug nozzles, see Ref. 42-45. Cold-flow tests showed that the effect of external flow on performance is confined to only a narrow range of external flow speeds with Mach numbers nearly unity.

Altitude compensation capability of plug nozzles for higher ambient pressures is indisputable. Since plug nozzles lose this capability for higher pressure ratios than the design pressure ratio, the latter should be chosen as high as possible. Taking this into account, plug nozzles will feature an even better overall performance than shown in Fig.6.1 and 6.2.
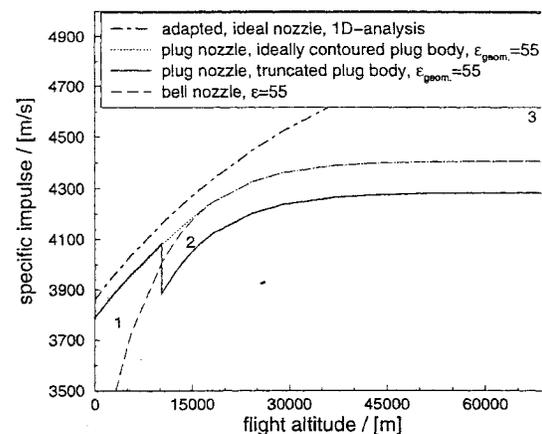
Fig. 6.2 : Performance characteristic of an ideal plug nozzle, a truncated plug nozzle, and a bell-type nozzle. Ideal expansion into ambience included for comparison.

17

Only for equal geometrical area ratios of plug nozzles and conventional bell nozzles, plug nozzles have worse high altitude performance due to truncation.

A plug nozzle is an integral part of the launcher. Ambient flow therefore may slightly influence the performance characteristic as long as the base flow is in open wake condition, see Section 5 for a detailed discussion. In contrast, a conventional engine with bell-type nozzle extension needs a thrust frame for engine integration. As this kind of engine layout cannot fill out the launcher base area, additional base drag is generated in case of ambient flow. This drag for a conventional bell-type engine nozzle should be taken into account for a fair performance trade-off between plug- and a conventional nozzle. The same holds actually also for the engine mass estimation.

7. CONTOUR DESIGN METHODS

Prepared by
Gerald Hagemann, and Hans Immich,
Astrium GmbH, Space Infrastructure Propulsion,
Munich, Germany

An ideally contoured supersonic flow nozzle produces an uniform, one-dimensional flow profile in the exit plane. The design philosophy is that at the design pressure ratio all expansion waves propagating through the flow towards the nozzle wall and thereby accelerating the flow to the desired design Mach number are cancelled out by a proper wall contour design.

The most simple design approach for the contour of a plug nozzle is based on a Prandtl-Meyer expansion around a corner for the throat inclination and also for the further contour definition. Figure 7.1 illustrates the principle of this approach, which was independently proposed by *Angelino*[6,34] and *Lee.*[35] A mass flow balance along each straight characteristic of the Prandtl-Meyer expansion fan finally defines the contour. Since this approach is purely based on the Prandtl-Meyer equations, it is however only fully valid for planar plug nozzle configurations with uniform, one-dimensional inflow.

To take into account the curved propagation of expansion waves for axis-symmetrical flow conditions, the method of characteristics has to be applied for the contour definition of a toroidal plug nozzle. This approach has also been proposed by *Angelino* in 1963, Ref.34. Further advantage of applying the method of characteristics is, that non-uniform inflow conditions through the throat or a primary internal expansion nozzle are taken into account. A detailed discussion on this is included in Ref. 77.

For high Mach number plug nozzles with sonic outflow though the throat and fully external expansion, large turning angles of the flow and thus of the throat are
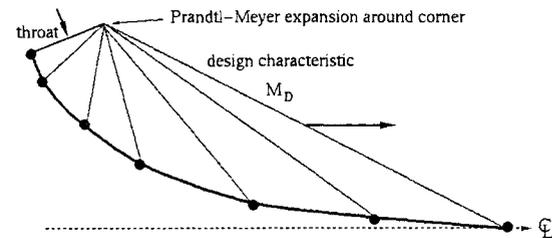
Fig. 7.1: Plug nozzle contour definition fully based on Prandtl-Meyer expansion fan around corner.
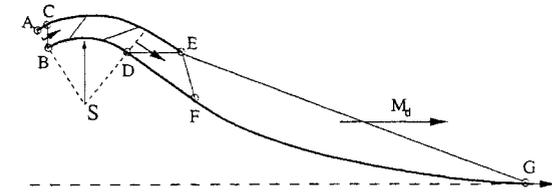
Fig. 7.2: Toroidal GSTP plug design with a combined internal and external expansion. Internal expansion in non-symmetric nozzle to Mach number, overall plug design Mach number M_D (cold air experiment).

required. As an example, the FESTIP linear plug model #1 tested within the frame of the ESA FESTIP programme by DaimlerChrysler Aerospace was designed for an exit flow with a Mach number of $M_D = 4.23$. For the purely external expansion with air, this requires a flow turning angle of approx. $\theta = 71°$, see e.g. References 8, 36, and 77 for further details.
A primary internal expansion may be realised to avoid the large turning angle, as it has been realised e.g. with the FESTIP plug model #2, the LION plug nozzle, and the GSTP toroidal plug nozzle, Ref.77.
For the GSTP plug tested within the frame of the ESA GSTP Programme by Volvo Aero Corporation at FFA in Sweden, a non-symmetric internal expansion nozzle producing a uniform, one-dimensional flow profile in the exit plane of the internal expansion nozzle was realised.[9]

Figure 7.2 gives details of the chosen design approach. The exhaust flow initially expands in the non-symmetric internal nozzle along the circular arc BD with the radius BS or SD to a Mach number of M_{id}. Along the internal exit characteristic DE, the flow is uniform. In the region DEF, this uniform flow is preserved, until then the external expansion takes place to the chosen exit Mach number of M_D. The contour DFG is defined based on the method of characteristics. Further details on the design are included in Ref. 77.

For truncated plug nozzles, an additional design approach was developed by *Rao,*[37] taking into account that a simple truncation of a plug nozzle with a full length central body for maximum performance does not automatically result in the best performing truncated plug nozzle. Therefore, *Rao* proposed a design method for truncated plug nozzles, based on a

18
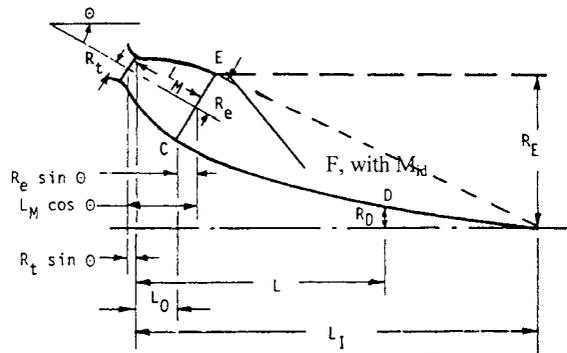
Figure 7.3:Geometry of a clustered plug nozzle.

variational method, similar to his well known method for shortened, thrust-optimised bell-type nozzles.[37]

To avoid any base flow development for truncated plug nozzles, non-optimised contours w.r.t. to performance could also be applied, e.g. conical plug bodies. As a plug engine is an integral part of a launcher, even a benefit w.r.t. to payload might be achieved due a potential decrease of engine mass with alternative contours, despite of their performance loss. In these approaches, the potential occurrence of flow separation due to the imperfect contours must be carefully studied.[29,41,54]

Major disadvantages of a toroidal plug nozzle with annular throat or a linear plug nozzle with a throat slot are:
- ➢ possible generation of side loads due to circumferential deviations of the throat gap as result of
  - tolerances in manufacturing of the nozzle hardware,
  - non-symmetrical thermal expansion during thrust chamber operation,
- ➢ maximum heat loads on large throat surface with tiny throat gaps
- ➢ control of combustion instabilities in the toroidal combustion chamber.
- ➢ No capability of thrust vector control by throttling of different sections of the throat.

Alternatively, clustered plug nozzles with several combustion chamber and primary nozzle modules were suggested to avoid the abovementioned shortcomings. Different design approaches for these clustered plug nozzles have been proposed in the literature, with conventional, bell-type nozzle modules, or with nozzle modules featuring a rectangular, 2-d exit cross section. The latter approach seems to be of advantage, since further losses induced by the gaps between individual modules, and due to the flowfield interactions downstream of the modules exits can be minimised. In principle, the flowfield development of a clustered plug nozzle with 2-d modules is similar to that of a toroidal plug nozzle, but with avoiding the inherent

disadvantages of the toroidal plug nozzle discussed above.

The following approximate approaches for the design of clustered plug nozzles with toroidal central plug body and conventional, bell-type primary nozzle modules are published in the literature:
- ➢ method of Aerojet (method 1), Ref. 38
- ➢ method of Aerojet (method 2), Ref. 38
- ➢ method of Rocketdyne, Ref. 39

For the design of the central plug body, all three approaches make use of the previously discussed methods of *Lee* or *Angelino*. The methods also have in common the definition of the outer ring with the individual bell-type module nozzles according to the following geometrical relationship, see e.g. Ref. 38 for further details. Figure 7.3 illustrates the different geometrical data and relationships.

8. AEROSPIKE: THRUST VECTOR CONTROL

prepared by
M. Calabrò, *EADS-LV*, Les Mureaux, France

Aerospike or plug nozzle may be envisaged for different applications such as:
- First stage of RLV or ELV (use of self-adaptability to ambient pressure),
- Upper or transfer stages (reason of use : short length and radial lay-out)

It may be used, as well with turbopumps or pressure fed engines, it can be axisymetric or bidimensionnal.

SPECIFICATIONS FOR TVC

Specifications will depend on the use:
- Winged 1st stage vehicle or SSTO :Generally speaking such a vehicle is implemented with 3 different kind of attitude control system :
  - An aerodynamic control operable with a maximum efficiency when maximum dynamic pressure occurs;
  - An RCS for reentry (high altitude and atmospheric flight over Mach about 2), so this ACS can be use for ascent in addition to the others ones, mainly for the high altitude phase. This RCS is completely independent of the propulsion system;
  - TVC of the main propulsion used only to trim and counteract the pitching moment, β max is limited by the capability of the chosen technology (some degrees :3 to 10+), this constraint have to be taken into account in the choice of the vehicle lay-out and on the trajectography analysis ,nevertheless slew rate could be lower than 5°/s.

Trade-off between use of these systems can be complex.

19

- For use on a conventional launcher (only one TVC), specifications are about, β max= 6° for a first stage with 10°/s of speed.

POSSIBLE TVC

Thrust vector control associated with Aerospike engines could be the same than on conventional rocket motors:
- Movable engine (totally or partly: some of the engines can be moved independently);
- Differential throttling between modules;
- Fluid injection in the divergent;
- Introduction of obstacles in the engine supersonic flow.

The state of the art on classical engines is to swivel the nozzle. For plug nozzles such methods are less attractive: TVC have to take into account that in general an Aerospike is used **only** with **liquid propellants**, the **engine** is made of a **cluster** of small ones[§] and that large plug nozzles have a diameter close to the launcher diameter, which makes gimballing the whole engine difficult and without any interest. As classical liquid engines have rather small diameters compared to the launcher diameter, the concentrated thrust is introduced into the launcher structure via a gimbal mechanism and a heavy thrust frame. The latter ensures that the thrust is evenly distributed into the launcher structure. By its nature, the plug nozzle already introduces the thrust in a distributed way into the launcher structure, so that the heavy thrust frame may be eliminated or at least may be reduced drastically in mass. This then calls for different methods to generate thrust vector control (TVC). TVC implies the 3 axis attitude control i.e. generation of pitch, yaw, and roll moments.

Retained solution has to be selected for its best compliance with the launcher architecture, the technological choices of the engine itself and the application (first or upper stage, turbopump or pressure fed) and with other TVC implemented systems.

TVC METHODS FOR PLUG NOZZLES

General Considerations
Classical liquid rocket motors use swiveling nozzles. This provides pitch and yaw control, but in case of a single engine, roll control is not possible. Multiple engines, as found on Ariane 4, Atlas booster stage, Titan, or Soyuz also allow for roll control. One main characteristic of these TVC ,their use do not induce specific impulse losses and are able to have good dynamic performances.

[§] In practice, pure annular plug nozzles cannot be used on large engines for two reasons: First, the throat width becomes very small, even for large booster engines leading to very difficult design and manufacturing problems. Second, heat transfer loads become prohibitive.
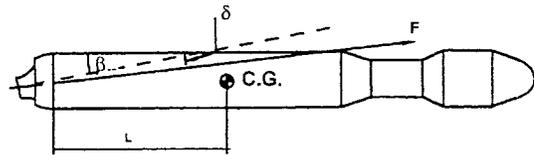
Fig.8.1: Movable Engine

Thrust Vector Control for Plug Nozzles

MOVING OF THE ENGINE
➤ **Whole Engine moving**
Swiveling the whole plug would lead to a heavier solution than differential throttling (for winged vehicles).This conclusion could probably be considered as general

➤ **Engine moving by units**
Nevertheless, thrust vector can be control by gimballing only some units (3-axis control needs 2 degrees of gimballing that is difficult to envisage whatever the launcher architecture could be) ; such a solution is not able to produce pure torques.

➤ **Central Plug swiveling**

Such a solution is by nature of low efficiency

FLUID INJECTION
Fluid injection could be an effective way of TVC and has been used on an old version of Titan launcher (2-axis control) and on military missiles (3-axis control on Russian Missiles: 8 tangential injection valves).
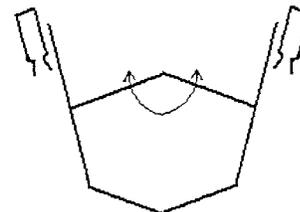
Fig.8.2: Movable Plug
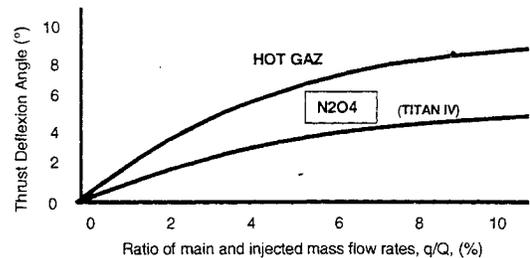
Fig. 8.3: Experimental thrust deflection angle for hot gas injection and for one reactive fluid (N_2O_4).

As atmospheric flight is very demanding in terms of $\int \beta.dt$ such a method is without interest when using another fluid than the same combustion products than

these of engine chamber (direct injection from chamber or gas produced by small engines) but such a solution - technically feasible-has never be developed for an operational use.

TVC BY DIFFERENTIAL THROTTLING

TVC may be achieved by reducing the chamber pressure in one nozzle and increasing the pressure in the opposite one (from one axis standpoint). The thrust of one nozzle is about proportional to the nozzle stagnation pressure.

- A first solution consist to have thrust variation of nozzles independently of the others:
  - Or turbopump(s) have to be dimensioned for maximum flow rate and pressure
  - Or separate booster pumps are implemented;
  This may not be cost or weight effective and also response times may become too long.
- Another option is to use throttling valves between two chambers fed by a common turbopump (no variation of overall mass flow rate).

The resulting moments are estimated by the contributions of the individual nozzles.

To accomplish TVC by thrust modulation, i.e., by reducing/ increasing the pressure in a set of individual combustion chambers, the cluster of individual combustion chambers has to be divided into four groups. For each of these groups, a throttling valve is required in the propellant feed lines, and in case booster pumps are used to increase the pressure, valves connecting the outlet(s) of the booster pump(s) to the injectors are required.

A single annular plug nozzle only allows for pitch and yaw control when using differential throttling. The linear plug nozzle allows for all three types of control, provided the upper and lower part of the plug have individually throttleable combustion chambers.
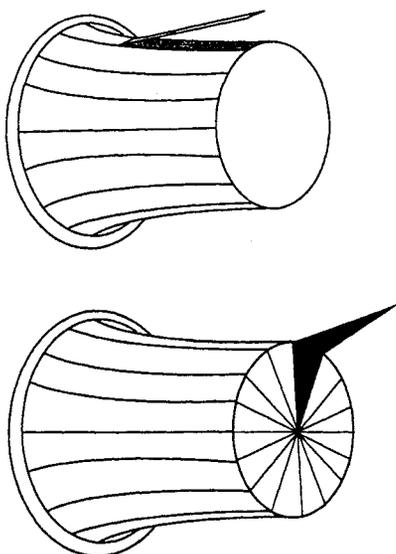
Fig.8.4: Schematic of flaps: on the plug or on the base area.

TVC Using Flaps

Vanes or obstacles are well-known means to accomplish TVC on launchers. The oldest launcher examples used vanes (German V-2 during World War II. American Scout launcher, ...). A disadvantage is that vanes are exposed all the time to the full impact of the hot combustion gases and can be eroded substantially during operation and reduce the performance of the rocket motor (losses of specific impulse). Flaps are exposed only when they are used and represent a better solution than vanes or than fluid injection, maintaining a β don't need any consumption of fluid; so, they may have some advantages in conjunction with plug nozzles.

Need of an accurate Parametric Model
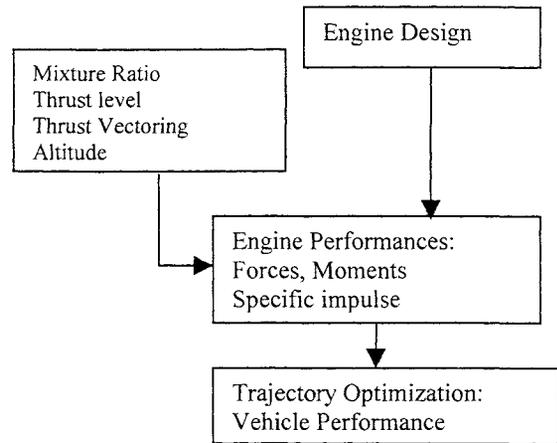
Launch vehicle performances are evaluated by computing the optimum vehicle trajectory under constraints; one part of the essential data for an accurate trajectory simulation is the engine performance.

The Aerospike engine performance is significantly more complex than a conventional engine since an Aerospike is capable of thrust modulation (plus variable mixture ratio and thrust level) and has a
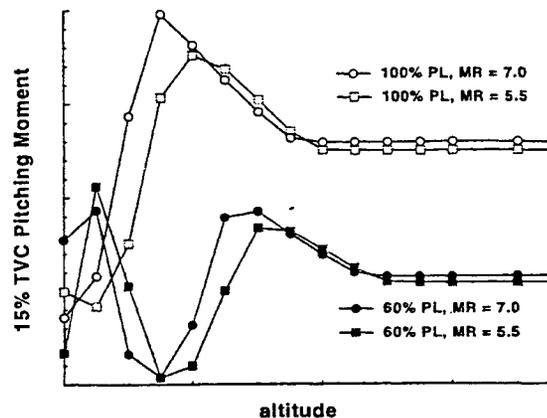
Fig 8.7: X33 Computed pitching moment for 15% thrust vector versus altitude for 2 power level and 2 mixture ratio ,Isp versus altitude

21

complex flow that interacts with the external aerodynamic and susceptible to operate or in "closed wake" or in "open wake" and perhaps to go from one to the other under external solicitations.

So, specific impulse delivered by the whole engine will depends of mixture ratio, thrust level, rate of throttling, vehicle attitude and altitude. Forces and moments (normal force, pitching moment) have a very nonlinear evolution at lower altitude and significantly different than in vacuum.

```
            ┌──────────────┐
            │  ON-BOARD    │
            │  MODEL       │
            └──────────────┘
┌──────────────────┐    ▲
│ GROUND TESTS     │    │   FLIGHT
│ VALIDATIONS      │    │   SIMULATIONS
└──────────────────┘    ▼
            ┌──────────────┐
          ▲ │  PARAMETRIC  │
            │  MODEL       │
            └──────────────┘
```
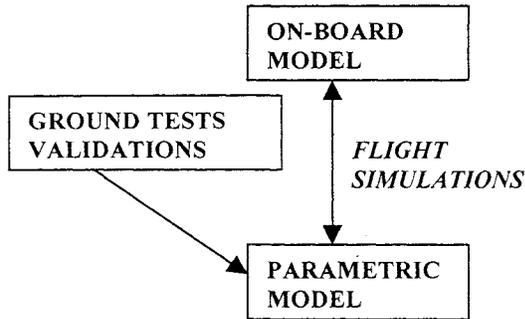
From control standpoint, on-board model have to be representative of a very complex reality –impossible to test on all the flight domain - with a certain level of accuracy. Flight simulations with the parametric model have to be done to check its validity; so the validation plan by tests of the parametric model is of first importance.

CONCLUSIONS

TVC methods for plug nozzles exists, they are able to meet the specifications in terms of $.\beta$ max (4 to 7 degrees for a first stage ,lower for an upper stage except if there is a non symmetrical payload); This allows the systems engineer to select the most attractive TVC system for a particular application for further detailed evaluation. The performance estimates and analyses have to be based on engineering models validated by a significant test program with altitude simulation. Due to the influence of altitude, it is not always possible to directly compare the TVC methods with each other. The moments of one given TVC that generate a side force or a thrust deflection angle depend on the (variable) position of the center of mass of the launcher.

For a linear plug, roll moments may easily be introduced by most methods. For differential throttling, it is necessary that there are at least four groups of independently throttleable combustion chambers: at the left and right side and at the upper and lower part of the linear plug, applicable for trim on winged vehicle.

A combination of canting and displacing the linear plug may provide for pitch, yaw, and roll moments. But displacement or canting of the plug is not

practicable for larger annular plug nozzles; Movables units seems possible for small upper stages

TVC METHOD	Comments	Performances
Movable Units	Needs independent roll control system, no-pure torques	
Hot Gas Injection	Complex, Roll control poss. with tangent valves, tech feasible, not applicable for trim	Fluid consumption, Is losses, High slew rate, limited βmax
Diff. Throttling	X33 Solution, 3-axis control with linear Aerospike but trim only	Limited dynamic with turbopump-fed engines, limited βmax
Flaps	Tech challenge , applicable for trim with losses	heavy(?), high βmax and slew rate

Direct hot gas injection has been demonstrated to be quite effective, It eliminates the need to store an additional fluid under high pressure but was never been operational on liquid engines and is probably not a solution for winged vehicle trimming.

Differential throttling has been implemented on X33, some experimental data seem to be available. Nevertheless, the method looks interesting for large linear plug nozzles.

Flap deflection, although also not investigated experimentally on plug nozzles, could have its interest but need to develop special technologies of hot composite movable panels, a detailed comparison with differential throttling have to be performed to determine if such a solution is of a real interest.

REFERENCES

[1] Ferri A,. "Improved Nozzle Test Techniques in Transonic Flow" AGARD AG-208, Oct. 1975

[2] Sacher P.W, "Aerodynamics of Aircraft Afterbody" AGARD AR-226, Jun. 1986

[3] Ch. Therry, "Aerodynamics of 3-D Aircraft Afterbodies" AGARD AR-318, Sep. 1995

[4] Nasuti, F. and Onofri, M., "Methodology to Solve Flowfields of Plug Nozzles for Future Launchers", *Journal of Propulsion and Power*, Vol. 14, No. 3, 1998, pp. 318–326, See also AIAA Paper 97–2941.

[5] Immich, H., Nasuti, F., Onofri, M., and Caporicci, M., "Experimental and Numerical Analysis of Linear Plug Nozzles", AIAA Paper 98–1603, Apr. 1998, 8th AIAA International Space Planes and Hypersonic Systems and Technologies Conference.

[6] Angelino, G., "Approximate Method for Plug Nozzle Design", *AIAA Journal*, Vol. 2, No. 10, 1964.

RTO-TR-AVT-007-V1

[7] Sutton, G. P., *Rocket Propulsion Elements*, John Wiley & Sons, New York, sixth ed., 1992.

[8] Hagemann, G., Immich, H., and Terhardt, M., "Flow Phenomena in Advanced Rocket Nozzles – The Plug Nozzle", AIAA Paper 98–3522, 1998.

[9] Olsson, J., "Investigation of Self-Adaptable Rocket Nozzles: External Expansion Nozzle", Study Note of Work Package 2.2, Detailed Test Plan, Rev.3, FFAP-A-1101, FFA, Oct. 1998.

[10] Onofri, M. and Nasuti, F., "ESA Technology and Research Projects: CFD Analysis of Plug Nozzles", Final Report, ESTEC/Contract n.12514/76/NL/FG, ESA/ESTEC, Noordwijk, The Netherlands, 1999.

[11] Sule, W. and Mueller, T., "Annular Truncated Plug Nozzle Flowfield and Base Pressure Characteristics", *Journal of Spacecraft*, Vol. 10, No. 11, 1973, pp. 689–695.

[12] Weiss, R. and Weinbaum, S., "Hypersonic Boundary-Layer Separation and the Base Flow Problem", *AIAA Journal*, Vol. 4, No. 8, 1966, pp. 1321–1330.

[13] Broglia, R., Di Mascio, A., Favini, B., Nasuti, F., Onofri, M., and Paciorri, R., "CFD Analysis of Axisymmetric Plug Nozzle Flowfields", ESTEC/Contract n.12019/96/NL/FG, Technology and Research Projects, ESA/ESTEC, Noordwijk, The Netherlands, Jul. 1997.

[14] Loth, E., Kailasanath, K., and Lockner, R., "Supersonic Flow over an Axisymmetric Backward-Facing Step", *Journal of Spacecraft and Rockets*, Vol. 29, No. 3, 1992, pp. 352–359.

[15] Tucker, P.K. and Shyy, W., "A Numerical Analysis of Supersonic Flow over an Axisymmetric Afterbody", AIAA Paper 93–2347, Jun. 1993, 29th AIAA/ASME/SAE/ASEE Joint Propulsion Conference.

[16] Nasuti, F., Paciorri, R., and Onofri, M., "Computation of Turbulent Supersonic Base Flows by a Shock-Fitting Quasi-Linear Solver", ASME Paper FEDSM99-7316, Jul. 1999, 3rd ASME/JSME Joint Fluids Engineering Conference.

[17] AA. VV., "ARPT – Advanced Rocket Propulsion Technology Program: Phase 3", Final Report, ESTEC/Contract n.12219/96/NL/FG – Phase 3.1, ESA/ESTEC, Noordwijk, The Netherlands, 1998.

[18] Nasuti, F. and Onofri, M., "Theoretical Analysis and Engineering Modeling of Flowfields in Clustered Module Plug Nozzles", *Journal of Propulsion and Power*, Vol. 15, No. 4, 1999, pp. 544–551, See also AIAA Paper 98–3524.

[19] Ruf, J. H. and McConnaughey, P.,K., "The Plume Physics behind Aerospike Nozzle Altitude Compensation and Slipstream Effect", AIAA 97-3217.

[20] Fick, M. and Schmucker, R. H., "Performance Aspects of Plug Cluster Nozzles", *Journal of Spacecraft and Rockets*, Vol. 33, No. 4, July-August 1996, pp 507-512.

[21] Sakamoto, H., Takahashi, M., Sasaki, M., Tomita, T., Kusaka, K. and Tamura, H., "An Experimental Study on a 14 kN Linear Aerospike-Nozzle Combustor", AIAA Paper-99-2761.

[22] Korst, H., "A Theory for Base Pressure in Two-Dimensional Flow and Comparison with Experiment", *J. Appl. Mech.*, No 23, pp. 593-600, 1956.

[23] Carrière, P. and Sirieix, M., "Facteurs d'influence du recollement d'un écoulement supersonique", 10th International Congress of Applied Mechanics, Stresa, Italy, 1960.

[24] Délery, J. and Lacau, R. "Prediction of Base-Flows", AGARD-FDP-VKI Special Course on "Missile Aerodynamics", March-April 1987.

[25] Reijasse, P., Benay, R., Délery, J. and Lacau, R., "Missile and Projectile Base-Flow Prediction by Multi-Component Methods", AIAA Paper 87-4380.

[26] Reijasse, P., Délery, J. "Multicomponent Approach for Propulsion Applications". European Seminar on Rocket Nozzle Flows, CNES, Paris, France, October 12-14, 1998; Proceedings Cnes/Dla/Sdt/Pl n 3003, November 1998.

[27] Tomita, T., Takahashi, M. and Tamura, T., "Flow Field of Clustered Plug Nozzles", AIAA Paper 97-3219.

[28] Tomita, T., Takahashi, M., Onodera, T. and Tamura, T., "Effets of Base-Bleed on Thrust Performance of a Linear Aerospike Nozzle", AIAA Paper 99-2586.

[29] Ito, T., Fujii, K. and Hayashi, A. K., "Computations of the Axisymmetric Plug Nozzle Flow Fields –Flow Structures and Thrust Performances", AIAA Paper 99-3211.

[30] Humphreys, R. P., Thompson, H. D. and Hoffmann, J. D. ,"Design of Maximum Thrust Plug Nozzles for Fixed Inlet Geometries", *AIAA Journal*, Vol. 9, No. 8, 1971, pp. 1581-1587.

[31] Lamb, J. P. and Oberkampf, W. L. ,"Review and Development of Base Pressure and Base Heating Correlations in Supersonic Flow", *Journal of Spacecraft and Rockets*, Vol. 32, No. 1, 1995, pp. 8-23.

[32] Onofri, M., Nasuti, F. and De Sio, M., "Engineering Analysis of the Nozzle Flow in CMPN", Advanced Rocket Propulsion Technology Final Presentation, ESTEC, Noordwijk, September, 1999.

[33] Fick M., "Performance Modeling and System Aspects of Plug Cluster Nozzles", AIAA Paper 98-3525, 1998.

[34] Angelino, G., "Theoretical and Experimental Investigation of the Design and Performance of a Plug-Type Nozzle", NASA TN-12, July 1963.

[35] Lee, C.C., "Fortran Programs for Plug-Nozzle Design", NASA TN R-41, March 1963.

[36] Immich, H. and Caporicci, M., "Status of the FESTIP Rocket Propulsion Technology Programme", AIAA Paper 97-3311, July 1997.

[37] Rao, G. V. R., "Spike Nozzle Contours for Optimum Thrust", *Ballistic Missiles and Space Technology*, Pergamon Press, New York, 1961.

[38] O'Brian, C. J., "Unconventional Nozzle Trade-Off Study", NASA CR-159520, 1979.

[39] N.N., "Advanced Aerodynamic Spike Configurations", Final Report, Rocketdyne, AFRPL-TR-67-246, 1967.

[40] Nasuti, F. and Onofri, M., "Analysis of In-Flight Behavior of Truncated Plug Nozzles", *Journal of Propulsion and Power*, Vol. 17, No. 4, pp. 809-817, 2001.

[41] Frey, M., and Hagemann, G., "Status of Flow Separation Prediction in Rocket Nozzles", AIAA Paper 98-3619, July 1998.

[42] Beheim, M.A., and Boksenbom, A.S., "Variable Geometry Requirements in Inlets and Exhaust Nozzles for High Mach Number Applications", NASA TM X-52447, 1968.

[43] Valerino, A.S., Zappa, R.F., and Abdalla, K.L., "Effects of External Stream on the Performance of Isentropic Plug-Type Nozzles at Mach Numbers of 2.0, 1.8 and 1.5", NASA 2-17-59E, 1969.

[44] Mercer, C.E., and Salters Jr., L.E., "Performance of a Plug Nozzle having a Concave Central Base with and without Terminal Fairings at Transonic Speed", NASA TN D-1804, 1963.

[45] Wasko, R.A., "Performance of Annular Plug and Expansion-Deflection Nozzles including External Flow Effects at Transonic Mach Numbers", NASA TN-D-4462, 1968.

[46] Erickson, C., "Thrust Vector Control Selection in Aerospike Engines", AIAA Paper 97-3307, July 1997.

[47] Schôyer, H. F. R., Hufenbach, B., Morel, R., Dalbiès, E., Immich, H., and Biggert, M., "Advanced Rocket Propulsion Concepts; Initial Considerations", Proceedings of the 16th Annual Aeroiet Paper No. C505/16/108, Inst. of Mechanical Engineers, London, Oct. 1995.

[48] Beichel, R., "Nozzle Concepts for Single Stage Shuttles", Astronautic and Aeronautic Vol. 13, No. 6, 1975, pp. 16-27.

[49] Dalbiès, E., "Thrust Vector Control", Advanced Rocket Propulsion Technologies, TN 4000, SEP, Vernon, France, March 1995.

[50] Morel, R., Dalbiès, E., Le Fur, T., Schöyer, H. F. R., Hufenbach, B., Immich, H., and Boman, A., "The Clustered Bell Aerospike Engine: Potential, Limitations and Preparation for Experimental Validation", International Astronautical Federation, IAF Paper 95-S.2.04, Oslo, Norway, Oct. 1995.

[51] "Engine Cooling", Advanced Rocket Propulsion Technologies, TN 3000, SEP, Vernon, France, Dec. 1995.

[52] ESA/ESTEC Bilan d'étude ARPT - Phase 1 - Mars 1994.

[53] ESA/ESTEC Bilan d'étude ARPT - Phase 2

[54] Rommel, T., Hagemann, G., Schley, C., Krulle, G. and Manski, D., "Plug Nozzle Flowfield Calculations for SSTO Applications", AIAA 95-2784-31st AIAA/ASME/SAE/ASEE Joint Propulsion Conference and Exhibit July 10-12, 1995/San Diego - CA

[55] Hagemann G., "Numerical Studies on 2D and 3D Plug Nozzle Configurations", Workshop on Plug Nozzles, DLR, Lampoldshausen, Germany, March 19, 1996. ESA-ESTEC, Noordwijk.

[56] Immich, H., Koelle, D. E. and- Parsley, R. C., "Plug Engine Systems for Future Launch Vehicle Applications", IAF-92-0647, 43rd Congress of the International Astronautical Federation, August 28 - September 5, 1992, Washington, DC, USA.

[57] Weegar, R. Understanding External Expansion Engines- LaunchSpace Magazine, August 1996.

[58] Fanciullo, T.J., Judd, D.C. and O'Brien, C. J., "Critical Engine System Design Characteristics for SSTO Vehicles", Journal of Spacecraft and Rockets, July 1996.

[59] Huang, D. H., "Aerospike Engine Technology Corporation for Space Propulsion" AIAA no 74-1080-AIAA/SAE 10th Propulsion Conference San Diego-October 21-23, 1974.

[60] Fuller, P.N. "Linear Rocket Engine Design Fabrication Testing" AIAA Paper 73-1179, 1973.

[61] French, J.V. and Chvanov, V. K., "NPO-The best of Both Worlds, A low cost, low risk US/Russian Reusable Launch Vehicle (RLV) Engine", -AIAA-Paper 95-3005, 1995.

[62] Baumgartner, R. I. and Elvin, J. D., "Lifting Body An Innovative RLC Concept", AIAA Paper 95-3531, 1995.

[63] Urie, D. M. and Elvin, J.D., "Advanced Development Company Innovative Economic Development and Technology for Single Stage To Orbit (SSTO) Concepts", AIAA Paper 95-0279, 1995.

[64] Dornheim, M. A., "Follow-on Plan Key to X33 Win", Aviation Week & Space Technology, July 8, 1996.

[65] Heald, D.A. "Plug Nozzle Propulsion System", General Dynamics Space Division System, San Diego, CA.

[66] Anfimov, N., "The Principle Directions of Russian Activities in Research for Conception of Future-Reusable Space Transportation System (The Program "ORYOL")", -AIAA-Paper 95-6003, 1995.

[67] Bekey, I., "SSTO rockets : a practical possibility", Aerospace America, July 1994.

[68] Lassmann, J. and Obersteiner , M., "Assessment Of Semi-Reusable Launcher Concepts", IAA Paper 96-V.3.0.3 - 47th International Astronautical Congress October 7-11, 1996/Beijing, China

[69] Schoyer, H .F. R., "Thrust Vector Control For (Clustered Modules) Plug Nozzles; Some Considerations", Journal of Propulsion and Power, Vol. 16 No. 2, March-April 2000.

[70] Korte, J.J., "Parametric Model of an Aerospike Rocket Engine", 38th Aerospace Sciences Meeting Jan 10-13, 2000/Reno, NV.

[71] Chang, P., Separation of Flow, Pergamon Press, Oxford, UK, 1970.

[72] Herrin, J. And Dutton, J., "Supersonic Base Flow Experiments in the Near Wake of a Cylindrucal Afterbody", AIAA Journal, Vol. 32, No.1, Jan. 1994, pp. 77-83.

[73] Benay, R. and Servel, P., "Applications d'un Code Navier-Stokes au Calcul d'Ecoulements d'Arrière-Corps de Missiles ou d'Avions", La Recherche Aerospatiale, No. 6, 1995, pp. 405-426.

[74] Amatucci, V.A., Dutton, J.C, .Kuntz, D.W., and Addy, A.L., "Two-Stream, Supersonic, Wake Flowfield Behind a Thick Base, Part I: General Features", AIAA Journal, Vol. 30, No. 8, 1992, pp.2039-2046.

[75] Tartabini P. V. "A Multidisciplinary Performance Analysis of a Lifting-Body SSTO", AIAA 2000-1045–38th Aerospace Sciences Meeting Jan 10-13,2000/Reno, NV.

[76] Calhoun P. "An Entry Flight Controls Analysis for a RLV", AIAA 2000-1046–38th Aerospace Sciences Meeting Jan 10-13,2000/Reno, NV.

[77] Hagemann, G., Immich, H., and Dumnov, G., "Critical Assessment of the Linear Plug Nozzle Concept", AIAA-2001-4865, July 2001.

[78] Hendershot, K., Sergeant, R., and Wilson, H., "A New Approach for Evaluating the Performance and Base Environment Characteristics of Nonconventional Rocket Propulsion Systems", AIAA Paper 67-256, Feb. 1967.